Optical Endpoint Detection for the Chemical Mechanical Polishing Process

by

Jamie Nam

B.S., Mechanical Engineering, 1998
Lehigh University

Submitted to the Department of Mechanical Engineering in partial fulfillment of the requirements for the degree of

MASTER OF SCIENCE IN MECHANICAL ENGINEERING

at the
Massachusetts Institute of Technology
January 2000
[February 2000]

© Massachusetts Institute of Technology 2000. All rights reserved.

Signature of Author..............................
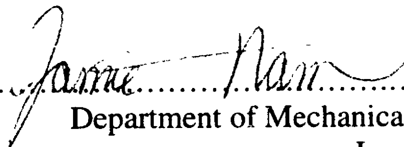
Department of Mechanical engineering
January 30, 2000

Certified by..............................
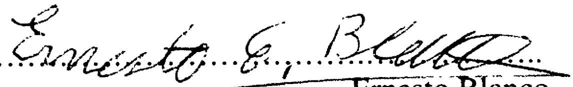
Ernesto Blanco
Adjunct Professor of Mechanical Engineering
Thesis Supervisor

Accepted by..............................
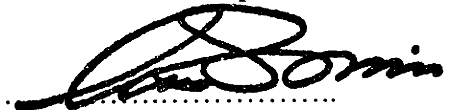
Ain A. Sonin
Chairman, Department Committee on Graduate Students

ARCHIVES

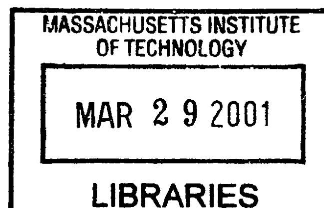
MASSACHUSETTS INSTITUTE OF TECHNOLOGY
MAR 29 2001
LIBRARIES

Optical Endpoint Detection for the Chemical Mechanical Polishing Process

by

Jamie Nam

Submitted to the Department of Mechanical Engineering
on January 30, 2000 in partial fulfillment of the
requirements for the degree of

Master of Science in Mechanical Engineering

Abstract

This thesis covers the design and implementation of a mechanism for detecting the endpoint for the Chemical Mechanical Polishing process of copper wafers. The proposed mechanism will detect the reflectance difference found in semiconductor materials to trigger the stop of the polishing process. This will prevent over polishing of the wafer while ensuring the optimal removal of excess materials. The mechanism is intended to run in-situ, while the polishing occurs. This is accomplished by embedding the reflectance sensor in the polishing platen to allow a clear view of the wafer surface. The reflectance from the surface of the wafer is a function of the material properties, surface structure, angle of incident light, and polarization of light. The experimental results revealed detectable change in the reflectance of the wafer surface, which may be used to determine the endpoint of polishing.

Thesis Supervisor: Ernesto Blanco
Title: Adjunct Professor of Mechanical Engineering

Acknowledgements

"Live life to the fullest and there will never be a dull moment."

Almost two years ago, I arrived at this prestigious university uncertain of what to expect. I knew it was going to be an experience to remember, whether good or bad. I believe you draw strength from your friends. Luckily, it didn't take long before we formed the "sweet" group. Thanks Andrew for your brotherly advice. You helped me make informed decisions about school and life. Corey, your stories and energy were stress relief for all of us. Gordon, you could always be depended upon. Mike, you always had the smile that infected the rest of us and also provided me with many rides—thanks!

Many thanks to Professor Ernesto Blanco, whose understanding and support made this time at MIT bearable. His vast knowledge and experience showed me the clear path to make the most of the time spent at this institution. I wish to thank Professor Jung-Hoon Chun, for the opportunity to take part in this research project. I would also like to thank Professor Nam P. Suh for the valuable advises that has given. Finally, I thank Dr. Saka, whose critical thinking and suggestions were helpful in honing many of my skills.

Aside from the "sweet" group, many people contributed to my sanity throughout this experience and to those I feel a deep sense of gratitude:

- to Tang for his wisdom and humor, you made the lab an interesting place to be.
- to Pankaj for his friendly innocence that can only come from TEXAS.
- to Micah, John, and George who laughed out loud.
- to my friend Laila, I am grateful for the friendship that developed so quickly. Your supporting words helped me more than you realize.
- to my most spiritual friend Shilpa who taught me many lessons in life without expecting anything back in return.
- to Akudo, the many late night conversations meant a lot to me.
- to Jason for his impressive understanding in many subjects. Thanks for your help.
- to Fardad and his willingness to listen. Maybe we can meet up at Café Astrata someday.
- to my parents who always gave me supporting words.
- to my younger sister Annie, who is sometimes mature beyond her years. You have taught me much about life and I love you, sis.
- to Lisa for her friendliness. I am eternally grateful for your help in proofing my thesis.
- to my young friend Amir who has taught me much. I appreciate all of your help throughout my time spent here.

Table of Contents

ABSTRACT 2

ACKNOWLEDGEMENTS 3

TABLE OF CONTENTS 4

LIST OF FIGURES 6

LIST OF TABLES 7

CHAPTER 1: OVERVIEW 8

1.1 INTRODUCTION 8
1.2 COPPER DAMASCENE PROCESS 9
1.3 COPPER CMP AND ITS PROBLEMS 12
1.4 ENDPOINT DETECTION SYSTEM 14
1.5 SCOPE OF THESIS 14
1.6 THESIS ORGANIZATION 15

CHAPTER 2: BACKGROUND AND EXISTING TECHNOLOGY 16

2.1 METROLOGY SCHEMES 16
2.2 EXISTING TECHNOLOGY 19
2.2.1 Mechanical Method 19
2.2.2 Electrical Method 20
2.2.3 Acoustical Method 23
2.2.4 Electrochemical Methods 24
2.2.5 Optical Methods 25
2.3 SUMMARY 27

CHAPTER 3: MODELING THE WAFER SURFACE REFLECTANCE 28

3.1 SURFACE EVOLUTION 28
3.1.1 Planarization Stage 29
3.1.2 Planar Surface Stage 30
3.1.3 Metal Clearing Stage And Endpoint 31
3.1.4 Dishing Stage 32
3.2 REFLECTANCE CHARACTERISTICS 33
3.2.1 Sinusoidal Surface 33
3.2.2 Flat Surface 36
3.2.3 Density Effect 36
3.2.4 Grating Surface 37
3.2.5 Over-polished Wafer Surface 38
3.3 REFLECTANCE FROM VARIOUS MATERIAL 39
3.4 EXPECTED REFLECTANCE SIGNAL TRENDS 39
3.4.1 Blanket Wafer Trends 39
3.4.2 Pattern wafer trends 40

CHAPTER 4: DESIGN AND IMPLEMENTATION 42

4.1 SENSOR REQUIREMENTS 42
4.2 SENSOR CHOICE 42
4.2.1 Axiomatic Design Decomposition 43
4.2.2 Philtec Sensor 43
4.3 IMPLEMENTATION INTO THE ALPHA MACHINE 45
4.3.1 Overall Machine Structure 46

4.3.2 *Integration of Sensor into Platen* ... 49
4.3.3 *Sensor Holder Design* ... 51
4.4 SYSTEM KINEMATICS ... 53
4.4.1 *Velocity Distribution* ... 53
4.4.2 *Sensor Position on the Wafer* ... 53
4.5 SENSOR VALIDATION ... 54
4.5.1 *Problems with the Test Bed Implementation* ... 55
4.5.2 *Differences Between the Alpha Machine and Test Bed* ... 56
4.5.3 *Similarities Between the Alpha Machine and Test Bed* ... 56

CHAPTER 5: EXPERIMENTAL RESULTS ... 57

5.1 SENSOR PERFORMANCE ... 57
5.1.1 *Material Property Testing* ... 57
5.1.2 *Effects of Slurry* ... 59
5.2 INCREMENTAL REFLECTANCE FROM PATTERNED WAFERS ... 61
5.3 TEST BED POLISHING DATA ... 62
5.3.1 *Experimental Parameters* ... 62
5.3.2 *Experimental Data* ... 63
5.3.3 *Comparing the Wafer Surface Condition with the Sensor Reading* ... 64
5.3.4 *Sensor Repeatability* ... 66
5.3.5 *Pattern wafer result* ... 66
5.4 SIGNAL ENDPOINT CHARACTERISTICS ... 67
5.4.1 *Threshold Comparison* ... 68
5.4.2 *Monitoring the Reflectance Change* ... 69
5.4.3 *Monitoring the Standard Deviation* ... 70
5.4.4 *Monitoring the Removal Rate* ... 71

CHAPTER 6: CONCLUSION ... 72

6.1 SUMMARY ... 72
6.2 POSSIBLE IMPROVEMENTS ... 73

APPENDIX A: AXIOMATIC DESIGN ... 75

APPENDIX B: SENSOR HOLDER DESIGN ... 83

REFERENCES ... 92

List of Figures

FIGURE 1.1 SINGLE DAMASCENE PROCESS ... 10
FIGURE 1.2 TOPOGRAPHY RESULTING FROM COPPER DEPOSITION ... 11
FIGURE 1.3 DUAL DAMASCENE DROCESS [2] ... 11
FIGURE 1.4 COPPER DEPOSITION AND CMP ... 12
FIGURE 1.5 IDEAL CASE AND REALISTIC CASE WITH EROSION AND DISHING ... 13
FIGURE 2.1 ILD POLISHING ... 16
FIGURE 2.2 SEQUENCES OF METROLOGY ... 18
FIGURE 2.3 MECHANICAL DETECTION SETUP ... 20
FIGURE 2.4 CONDUCTIVE MEASUREMENT SETUP ... 21
FIGURE 2.5 IMPEDANCE MEASUREMENT SETUP ... 22
FIGURE 2.6 CAPACITANCE MEASUREMENT SETUP ... 22
FIGURE 2.7 ACOUSTICAL DETECTION SETUP ... 23
FIGURE 2.8 ELECTROCHEMICAL DETECTION SETUP ... 24
FIGURE 2.9 OPTICAL DETECTION SETUP (SCATTERING) ... 25
FIGURE 2.10 OPTICAL DETECTION SETUP (REFLECTANCE) ... 26
FIGURE 3.1 WAFER SURFACE PROFILE AFTER COPPER DEPOSITION ... 30
FIGURE 3.2 PICTURE OF PATTERNED WAFER (BEFORE POLISHING) ... 30
FIGURE 3.3 WAFER SURFACE AFTER PLANARIZATION ... 31
FIGURE 3.4 PICTURE OF PATTERNED WAFER (CLOSE TO PLANARITY) ... 31
FIGURE 3.5 WAFER SURFACE AT ENDPOINT ... 32
FIGURE 3.6 PICTURE OF PATTERNED WAFER (AT ENDPOINT) ... 32
FIGURE 3.7 WAFER SURFACE WITH OVER-POLISHING ... 33
FIGURE 3.8 SINUSOIDAL SURFACE STRUCTURE ... 34
FIGURE 3.9 MAGNITUDE VALUE OF BESSEL FUNCTION ... 35
FIGURE 3.10 SPECULAR REFLECTANCE ... 36
FIGURE 3.11 EQUIVALENT DIFFRACTION CONFIGURATION ... 37
FIGURE 3.12 DIFFRACTION CHARACTERISTICS ... 38
FIGURE 3.13 DIFFRACTION FROM ROUGH GRATED SURFACE ... 38
FIGURE 3.14 REFLECTANCE PROPERTY OF COMMON MATERIALS ... 39
FIGURE 3.15 REFLECTANCE CHARACTERISTICS OF A BLANKET WAFER ... 40
FIGURE 3.16 REFLECTANCE CHARACTERISTICS OF A PATTERNED WAFER ... 41
FIGURE 4.1 PHILTEC SENSOR CHARACTERISTIC ... 44
FIGURE 4.2 SENSOR'S INTERNAL COMPONENTS ... 45
FIGURE 4.3 ALPHA CMP MACHINE ... 46
FIGURE 4.4 GRANITE LOWER STRUCTURE ... 47
FIGURE 4.5 GANTRY UPPER STRUCTURE ... 48
FIGURE 4.6 CARRIER ASSEMBLY ... 49
FIGURE 4.7 SENSOR IMPLEMENTATION ... 50
FIGURE 4.8 VERTICAL ADJUSTMENT MECHANISM ... 51
FIGURE 4.9 SENSOR HOUSING ... 52
FIGURE 4.10 COORDINATE SYSTEM OF THE ROTARY CONFIGURATION ... 54
FIGURE 4.11 TEST BED POLISHING MACHINE ... 55
FIGURE 4.12 TEST BED MODIFICATION ... 56
FIGURE 5.1 TEST BENCH SETUP ... 58
FIGURE 5.2 TEST BED MODIFICATION ... 60
FIGURE 5.3 REFLECTANCE OF 0.5 μM LINES AT 50% DENSITY ... 62
FIGURE 5.4 BLANKET WAFER POLISHING (AVERAGED OVER WAFER) ... 63
FIGURE 5.5 BLANKET WAFER POLISHING (SCANNED OVER WAFER) ... 64
FIGURE 5.6 CORRELATION BETWEEN SENSOR SIGNAL AND PHYSICAL WAFER CHARACTERISTICS ... 65
FIGURE 5.7 MULTIPLE BLANKET WAFER POLISHING RESULTS ... 66
FIGURE 5.8 PATTERN WAFER POLISHING RESULTS ... 67
FIGURE 5.9 THRESHOLD DETECTION FLOW CHART ... 68
FIGURE 5.10 THRESHOLD COMPARISON ... 69

FIGURE 5.11 CHANGE IN SIGNAL DETECTION 70
FIGURE 5.12 DETECTION BY MONITORING STANDARD DEVIATION 71

FIGURE A. 1 ASSEMBLY EXPLODED VIEW OF SENSOR HOLDER 84
FIGURE A. 2 SENSOR HOUSING 85
FIGURE A. 3 POSITIONING NUT 86
FIGURE A. 4 SENSOR TIP 87
FIGURE A. 5 SENSOR RESTRAINING KEY A 88
FIGURE A. 6 SENSOR RESTRAINING KEY B 89
FIGURE A. 7 LOCKING MECHANISM 90
FIGURE A. 8 WALL MOUNT 91

List of Tables

TABLE 4.1 PHILTEC SENSOR SPECIFICATIONS 45
TABLE 5.1 REFLECTANCE OF VARIOUS MATERIAL 58

Chapter 1: Overview

1.1 *Introduction*

The semiconductor industry supplies the world with integrated circuits (ICs) necessary to produce computers and other electronic devices. Over the past decade, microprocessors and other devices have become much faster and much more reliable. Today, these advances have facilitated the design of extremely small features on the IC chips that seemed impossible only a few years ago. This was accomplished by introducing both new advanced materials as well as new processes.

Aluminum is currently used as the main interconnect material that connects the devices on a chip. However, copper is quickly gaining acceptance as the on-chip conductor of the future. The reason for this switch to copper is because of its lower resistance. Copper has a resistance of less than 2 μΩ-cm while aluminum has a resistance of over 3 μΩ-cm [1]. The lower resistance of copper is essential for the optimal functioning of a high performance microprocessor. It also reduces the power consumption of integrated circuit chips.

Aluminum shows poor immunity to electromigration, making it ineffective in handling higher power densities. Using copper resolves this problem and increases the reliability of the interconnect lines. The final advantage of using copper over aluminum can be seen from the manufacturing perspective. Aluminum requires complicated metal etching and oxide polishing. However, since copper is difficult to etch, a new process called "damascene" has been developed. This process requires 20-30% fewer steps than the traditional subtractive patterning method seen with aluminum. Furthermore, the use of copper allows smaller lines to carry the same amount of current so that higher density

features can be designed. This means fewer layers are needed to achieve the connections that would have been necessary for aluminum interconnects. Therefore, a substantial reduction in manufacturing cost can be achieved by using copper.

1.2 *Copper Damascene Process*

In the conventional metalization process, aluminum is deposited on the inter-layer dielectrics (ILD), and then patterned and etched to form the interconnection lines. For copper, an alternative deposition method called "the damascene process" has been developed. In this technique, ILD is first deposited on the substrate. The ILD is then patterned to form trenches where metal interconnect lines lie. Afterwards, copper is uniformly deposited on the wafer surface to fill the trenches. Excess material is polished away using chemical-mechanical polishing (CMP).

The damascene process eliminates the difficult metal etching process and promotes better control of oxide critical-dimension patterning (rather than metal patterning). It also eliminates the need to polish a dielectric layer multiple times to form the interconnect lines. Consequently, this reduces the overall cost and processing time.

There are two main categories of the damascene process: single and dual damascene. Single damascene requires the ILD deposition, patterning, metal deposition, and polishing sequence to be completed twice to achieve the interconnect lines as shown in Figure 1.1.

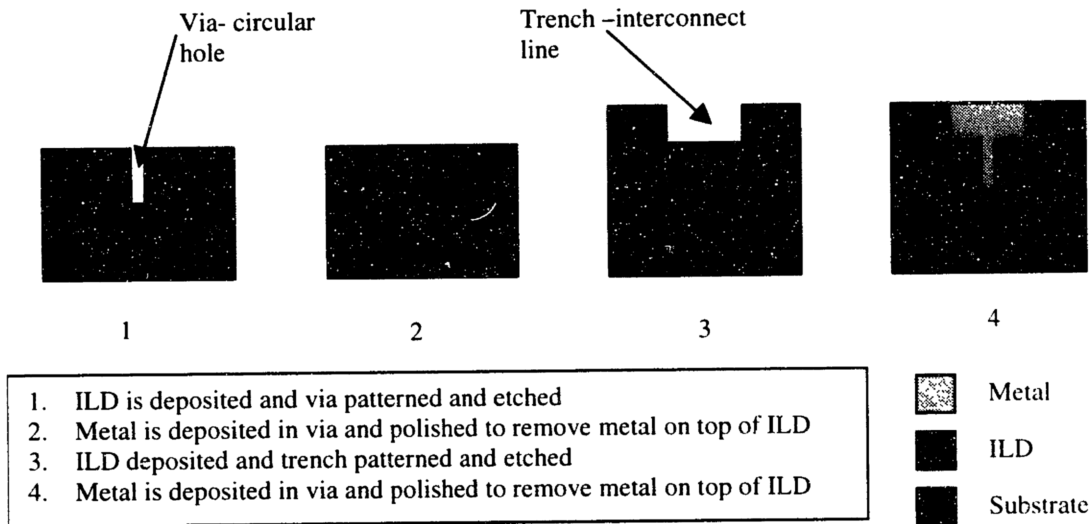

Figure 1.1 Single Damascene Process

However, the dual damascene process completes the two sequences simultaneously. There are three ways to complete the dual damascene process. Each of them results in the same structure as seen in Figure1.1. They differ in their sequences of "via" and trench patterning and etching. "Via" is a circular hole that connects the device (on the substrate) to the interconnecting lines. The three different approaches are "buried-via," "trench-first," and "via-first." Dual damascene processes are shown in Figure 1.3 [2]. In the "buried-via" approach, a hard mask is patterned and etched. Trenches and via's can then be etched in one step. The drawback of this approach is the extreme difficulty of getting good alignment of the trenches with the holes in the hard mask. The "trench-first" approach patterns the via after the trench has been etched. This method can be difficult because of the thick layer of photo-resist that lithography must overcome. Perhaps the best solution is the "via-first" approach. For this method, an intermediate etch stop layer is required to define the trench. Without it, the edges can be rounded during the etching process and the depth of the trenches may be hard to control. Once the

trench and via are formed, the copper is deposited on the surface to fill these structures. The resulting topography is a strong function of the trench structure and the deposition process. Therefore, it is difficult to predict the exact topography after deposition. However, from available literature, it appears that a sinusoidal surface profile is achieved when the pattern density is near fifty- percent with small line widths. The land areas of the ILD become the crests on the copper surface and likewise, the trench features cause the troughs as shown in Figure 1.2.

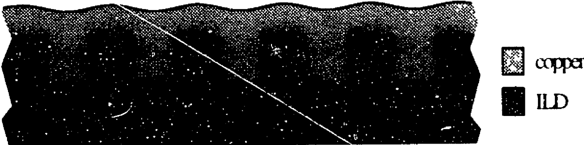

Figure 1.2 Topography Resulting from Copper Deposition

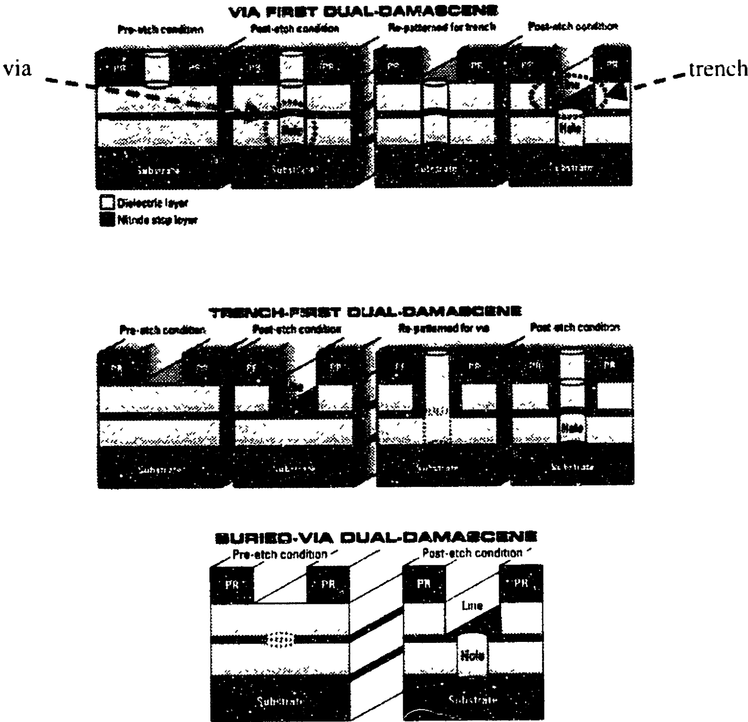

Figure 1.3 Dual Damascene Drocess [2]

1.3 *Copper CMP and Its Problems*

The chemical mechanical polishing (CMP) process is used extensively in the semiconductor industry to polish away a thin layer of material from the surface of a wafer [3]. The emerging technology polishes the copper surface rather than the ILD surface, which was traditionally used for aluminum interconnects.

Prior to copper CMP, trenches were formed in the oxide layer. Thereafter, the copper was deposited over the entire wafer to fill these trenches. The top layer of copper was then polished away to leave metal only in the trenches and via's with the land area clear of any conducting metals.

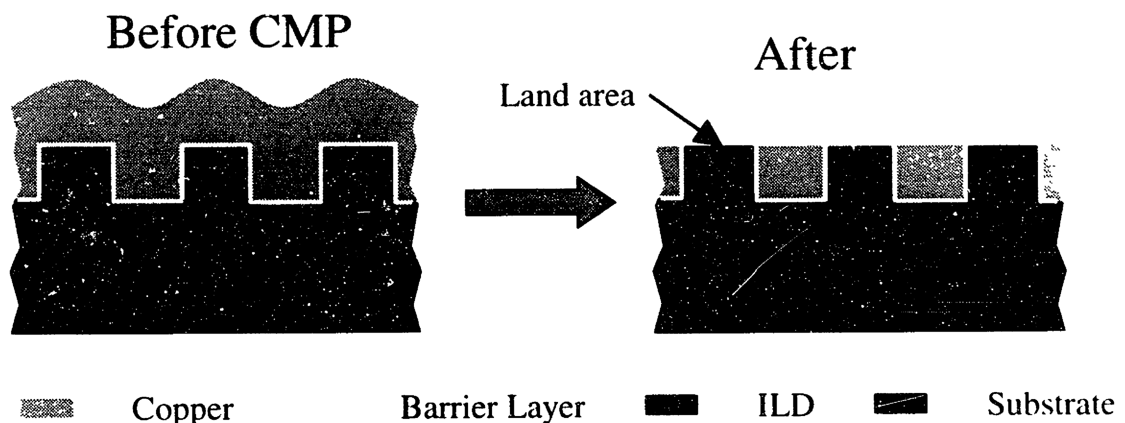

Figure 1.4 Copper Deposition and CMP

Ideally, the process should leave the surface perfectly flat. However, polished wafers may suffer from non-ideal effects such as dishing and erosion caused by CMP. These effects can be seen in Figure 1.5 where a cross-sectional view of the ideal polished endpoint is compared to the more realistic case, which suffers from dishing and erosion. Dishing is defined as the recess height of the copper layer as compared to the neighboring oxide layers. Erosion, on the other hand, is defined as the height of the polished oxide,

measured from its original height. Dishing can be present in the eroded region, where it is still measured as the most recessed copper level as compared to the surrounding eroded oxide region, not to the original oxide height.

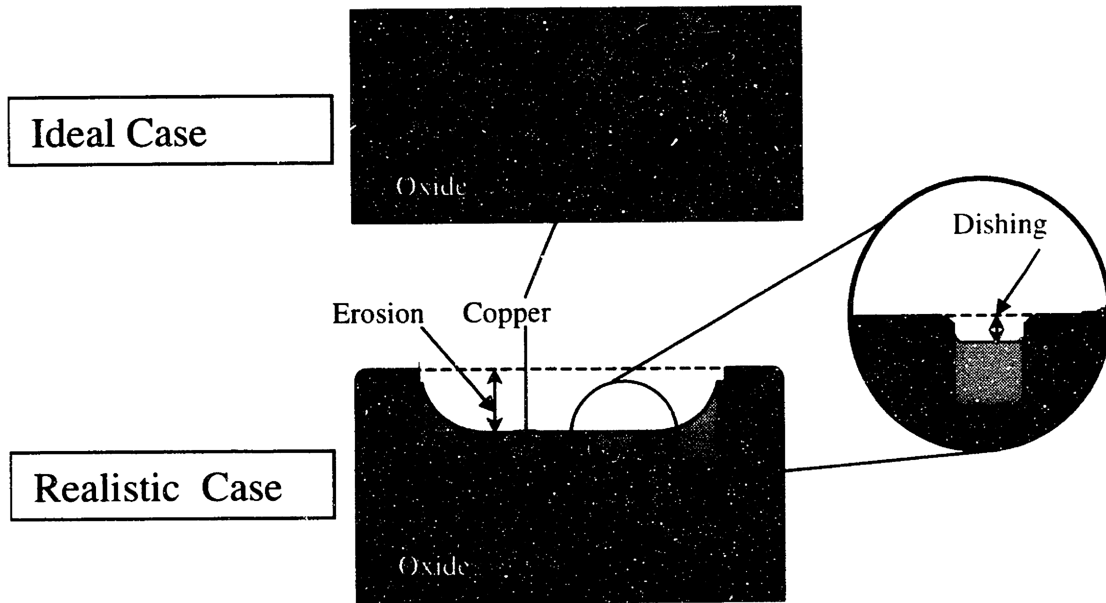

Figure 1.5 Ideal Case and Realistic Case with Erosion and Dishing

The non-ideal effects of dishing and erosion can limit chip design and performance. Today, wafers may have as many as twelve layers of interconnects. This means that planarity error from one layer to the next would result in the top layers having high topographic features that would make focusing difficult for lithography. Furthermore, the pattern dependent variations in line thickness severely affect the resistance of copper and may result in circuit performance degradation.

1.4 *Endpoint detection system*

Oxide and metal polishing endpoints are defined differently. For oxide polishing, the endpoint is the state when the oxide layer is planar and has reached the desired thickness, whereas in metal polishing, the endpoint is defined as the state when *all* of the metal is removed from the insulating land areas, leaving metal only in the trenches.

The ability to determine the end of polishing, before the onset of dishing and erosion, is highly beneficial. Previously, much of the endpoint detection was time-based and determined only by trial and error runs. This can be very costly, especially if the process parameters drift, resulting in different polishing times. Ideally, a measured variable would indicate the polishing endpoint. This would increase the overall performance of the CMP machine and prevent many of the problems associated with this process.

The idea behind endpoint detection is to identify a variable that changes drastically during the polishing process. Presently, there are existing technologies exploiting electrical, optical, and mechanical characteristics to determine the endpoint.

1.5 *Scope of thesis*

This thesis will evaluate the present detection methods and the potential methodology for detecting the endpoint of the polishing process. The central focus of this thesis is to develop and implement a detection method for metal polishing in a CMP machine. Certain polishing characteristics will be modeled, however, it must be kept in mind that the polishing process is complex, and an exact understanding of it is yet unknown. Therefore, the majority of the detection work will be empirically based.

1.6 *Thesis Organization*

This thesis consist of five parts: In Chapter 2, a brief overview and background of the existing technology will be presented. This chapter also describes the various metrology schemes to measure wafer surface characteristics, and reviews the variables that change during polishing. Examples of measurement techniques will also be discussed. Chapter 3 reviews how the reflectance is affected by surface topography and material compositions. The fourth chapter describes the design and implementation of an endpoint sensor into the polishing machine, while Chapter 5 shows experimental results collected from the sensor. Finally, Chapter 6 summarizes the work of this thesis, discusses the limitations of the detection method, and suggests possible improvements.

Chapter 2: Background and Existing Technology

Section 1.3 defines the metal CMP endpoint as the state when all of the metal from the wafer surface has been removed, leaving metal only in the trenches. Initially, the wafer surface is rough, because of topography resulting from the inlaid trench geometry. During polishing, the top metal layer is removed, exposing the oxide land areas. This results in a surface with a composition of various materials such as copper and SiO_2. The change in surface quality and material may be monitored to detect the endpoint. The emphasis in this thesis is to identify metal polishing characteristics. However, it is important to look at the more traditional ILD polishing characteristics to understand the complete background of the existing technologies. During this polishing, there is no transition in material properties. Rather, only ILD is polished from a rough surface to a planar surface that has the desired thickness.

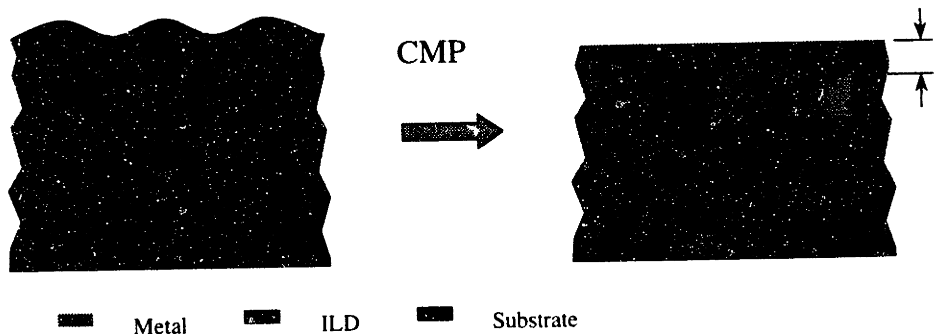

Figure 2.1 ILD Polishing

2.1 *Metrology Schemes*

There are three metrology schemes to measure the wafer surface quality [4]. They differ in their sequence of measuring and polishing the wafer surface. The off-line,

inline, and in-situ metrology schemes are shown in Figure 2.2. The traditional off-line scheme uses a stand-alone (SA) metrology tool that sits outside of the polishing machine. This metrology tool measures and verifies the removal rate and surface quality of a full wafer batch while another batch is being polished. The SA system has excellent capability to provide full and accurate information about the wafer surface characteristics. However, this off-line scheme is not the best solution for the manufacturing environment. It requires a complex run to run control algorithm, based on SA measurements, that is less effective in the dynamic CMP process. This dynamic process has high dependencies on the product type and the materials involved, as well as polishing parameters that require real time response capabilities. If error occurs during polishing, a full batch of wafers may be over-polished before recognition of a problem.

The in-line scheme therefore has the measurement tool installed in the polishing system. This device has full metrology capabilities similar to the stand-alone system. It combines the performance of an SA tool and responds quickly to polishing changes by measuring every polished wafer. The wafer is measured immediately after polishing, while still within the equipment environment. This gives the option of re-polishing the under-polished wafer immediately. The dynamic nature of the CMP process is quickly compensated so those problems do not alter the yield.

The off-line and in-line metrology methods can measure the wafers only after complete polishing. However, if polishing characteristics change while the wafer is still in the CMP machine, it may sacrifice a number of wafers before the problem is identified and solved. For this reason, the in-situ detection method is very desirable. It allows the measurement tool to constantly monitor the wafer, while polishing, for the fastest

response to any changes in the polishing machine. The understanding of how the wafer is polished may be used to control the polishing parameters for the optimal removal of the metal. Figure 2.2 shows the various configurations that have been discussed.

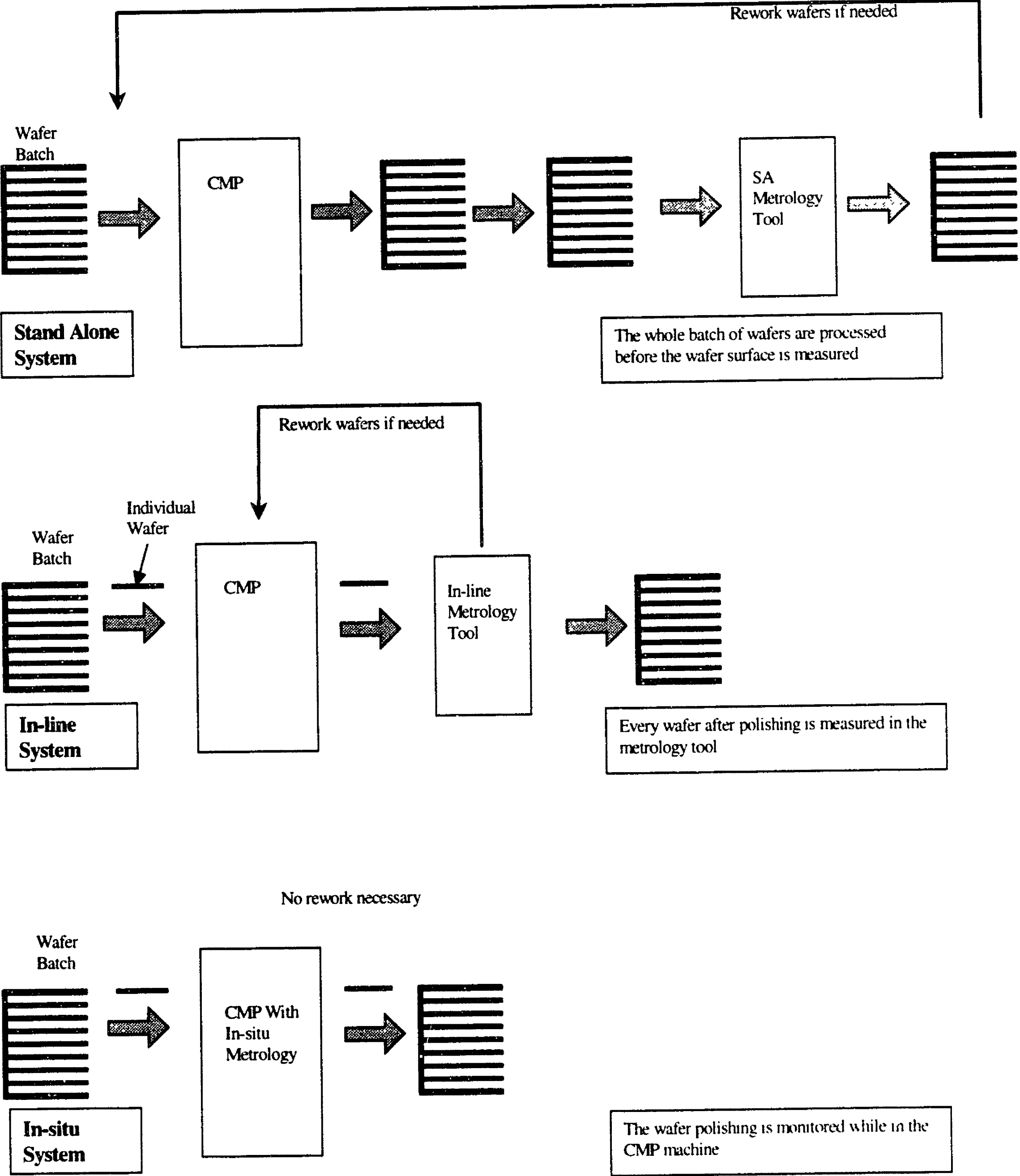

Figure 2.2 Sequences of Metrology

To ensure that the measurement tools are working properly, it may be necessary to use multiple schemes to verify their performance. For example, if an in-situ sensor is used, an in-line metrology tool can provide feed back of the sensor's performance. This results in a very reliable and fast responding detection system.

2.2 ***Existing technology.***

This section gives an overview of the currently implemented endpoint detection methods as well as some proposed techniques. There are five variables that can be measured to determine the end of polishing. These are mechanical, acoustical, chemical, electrical, and optical characteristics [5].

2.2.1 Mechanical Method

The mechanical detection method measures the change in the friction coefficient in the polishing interface [6]. This method is ideal for detecting metal polishing because the surface composition changes from all copper to a combination of copper and oxide. This results in a friction change that can be measured. However, in ILD polishing, there is no material composition change. Rather, the sensor monitors the roughness of the top ILD layer as seen in Figure 2.2. When the friction decreases, it indicates that the surface is planar and the polishing is stopped. This method of determining the endpoint is desirable compared to many of other detection schemes because there is no need to contact the wafer surface that may cause scratching.

The friction force resulting from polishing wafers can be measured by monitoring the current load on the platen motor as seen in Figure 2.3. Similarly, a load cell can measure the horizontal load on the wafer carrier spindle. This also indicates the friction force in

the polishing interface. The load cell measurement is a more direct measure of the friction force and may reduce the noise in the signal compared to the motor current measurement. Both of the configurations in Figure 2.3 measures the friction over the entire wafer surface. This measurement method is easy to implement. However, noise from the polishing interface reduces the sensitivity of this detection method. Furthermore, this method is not very sensitive to surface planarity changes that reduce the effectiveness when measuring ILD layer polishing.

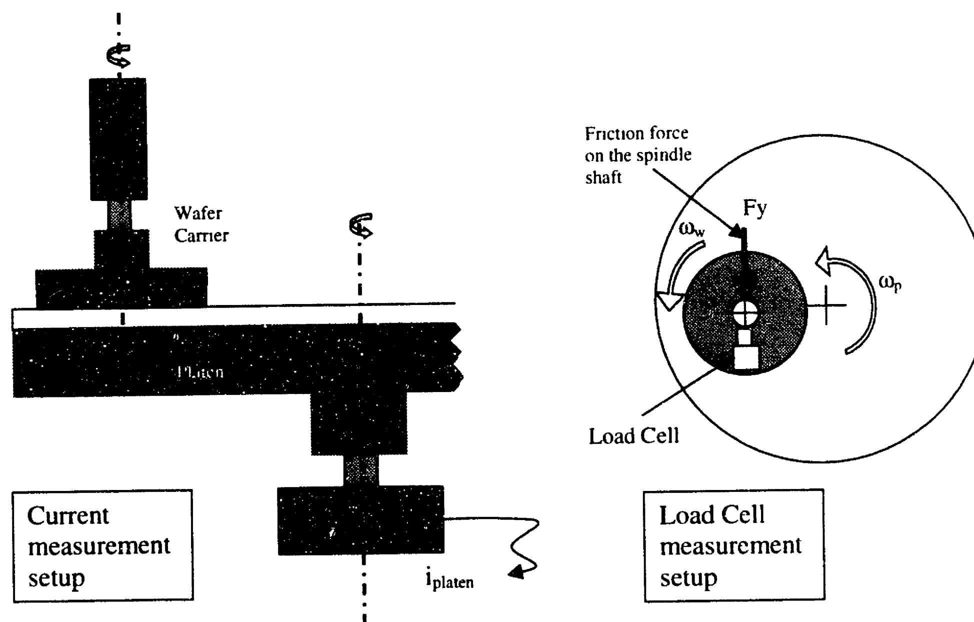

Figure 2.3 Mechanical Detection Setup

2.2.2 Electrical Method

The previous section explores measuring the electrical current characteristics from the platen motor for detecting the endpoint of polishing. However, conductivity, capacitance and impedance characteristics of the wafer may also be used to indicate the endpoint. During metal polishing, the excess metal on the wafer surface allows the current to pass between two electrodes, as seen in Figure 2.4. However, as soon as the metal clears, the

conductivity of the wafer surface decreases, which indicates the endpoint [7]. For ILD polishing, the opposite occurs. The ILD layer must be completely removed, exposing the network of conducting lines, which allows current to pass through. The conduction method is not feasible because of the concerns of causing damage to the wafer. First, the sensor requires contact with the wafer surface that may cause scratches. Second, there is a risk of damage caused by passing current through unprotected devices. Finally, there are connection reliability concerns between the sensor electrodes and the wafer that make this method unfeasible.

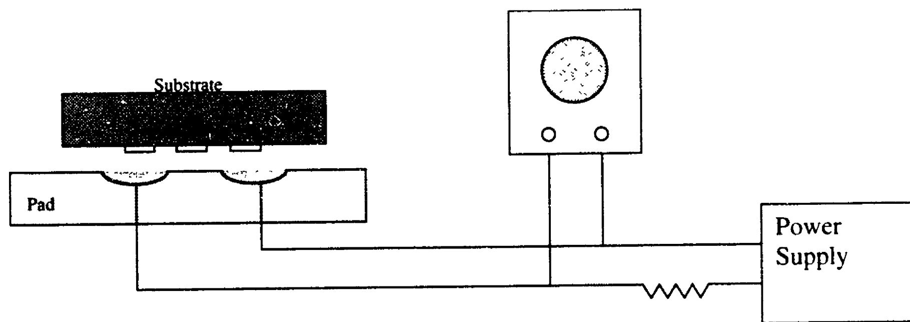

Figure 2.4 Conductive Measurement Setup

Another detection method measures the impedance change of the wafer surface during polishing as shown in Figure 2.5 [8]. It requires electrical contact with the conductive wafer surface. The leads are then connected to a coil that rotates with the platen. A second coil that is stationary and energized allows the rotating coil to pass through an air gap in the high permeable core. The resulting flux field in the gap is a function of the resistance on the wafer surface. Similar to the conductive method, measuring impedance requires connection to the wafer that may pose reliability and wafer scratching problems.

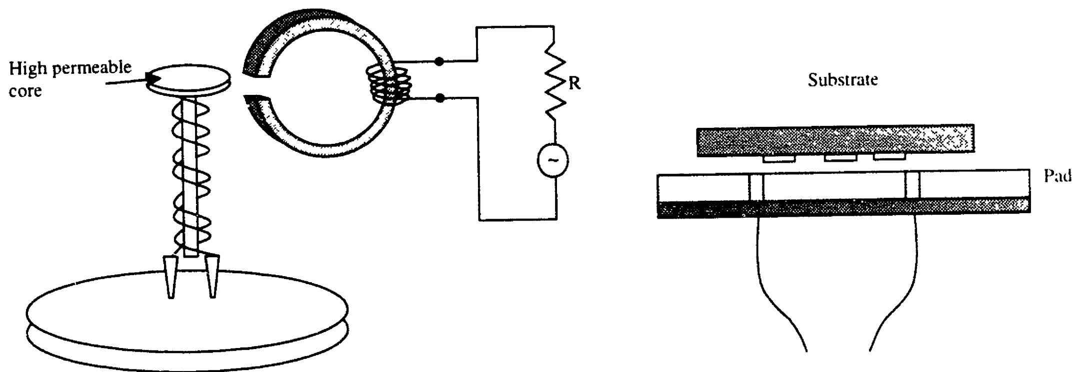

Figure 2.5 Impedance Measurement Setup

Finally, the capacitance characteristic of the wafer surface can indicate the dielectric thickness as the wafer is polished as seen in Figure 2.6 [9]. This is accomplished by forming a constant current source and monitoring the associated voltage across the dielectric film. The capacitance sensor is embedded into the platen and will not scratch the wafer surface. The electronic circuitry is designed to produce an output that is inversely proportional to the dielectric layer thickness. This method claims to monitor uniformity variations on the wafer surface. It saw considerable success on blanket wafers, however, patterned wafers have been more difficult to characterize.

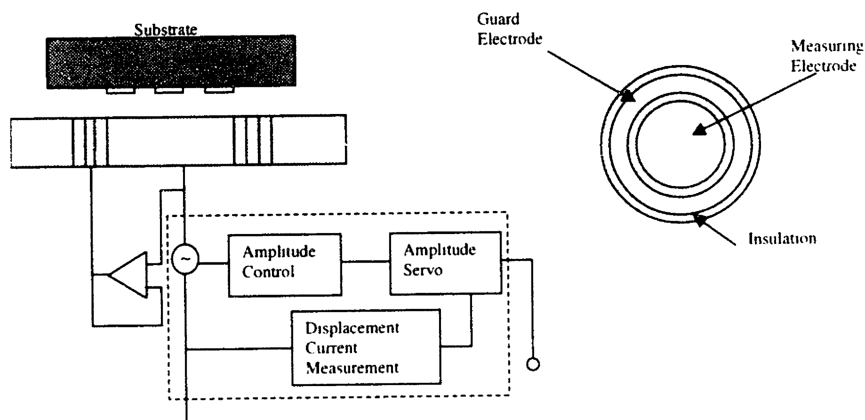

Figure 2.6 Capacitance Measurement Setup

Most electrical schemes are invasive and can cause damage to the wafer surface when contact with the surface is required. Therefore, this problem must be addressed before any of these methods can be implemented to detect the endpoint.

2.2.3 Acoustical Method

This method monitors the sound created by the grinding action that takes place during polishing. The measured acoustical signal can be analyzed to determine the change in amplitude and the frequency of spectral peaks depending on the surface condition [10]. In ILD polishing, the acoustic signature measures the change in thickness of the layer being polished. However, when polishing dissimilar materials, the acoustic signature changes in a measurable way when the interface is exposed. The problem with this method is the noise produced by the CMP process. Motors and other mechanical systems produce noise that interferes with the detection method. It requires extremely complex signal processing that prevents this method from being feasible for production.

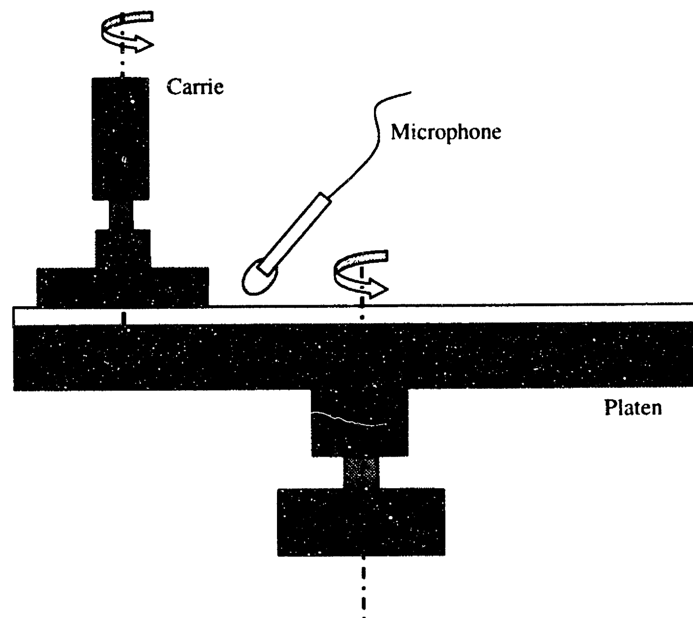

Figure 2.7 Acoustical Detection Setup

2.2.4 Electrochemical Methods

This method detects the difference in potential between a measurement electrode and a reference electrode [11]. The measurement electrode can be the surface of the wafer or a probe inserted in the slurry nearby. The measured potential depends on the properties of the materials involved during polishing. Therefore, the surface transition from bulk metal to the barrier layer and from the barrier layer to the underlying oxide can be measured.

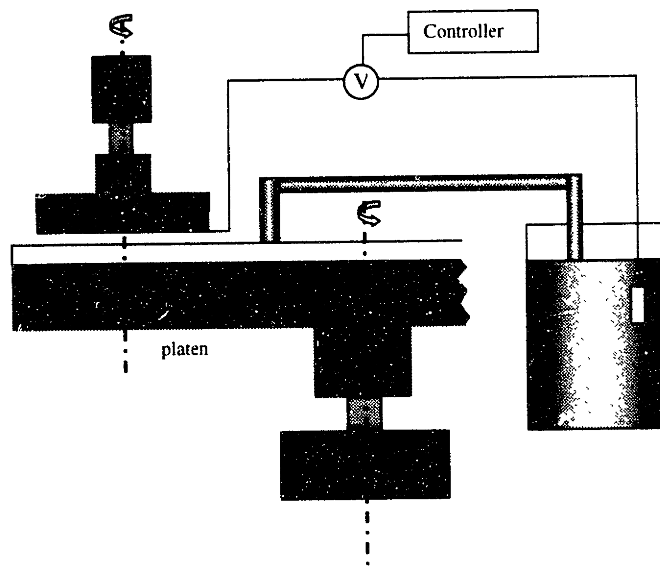

Figure 2.8 Electrochemical Detection Setup

It is more desirable to measure the properties of the slurry rather than the wafer surface to prevent damaging the wafer. However, measuring the slurry may present unwanted results. The polishing pad is a microporous polyurethane material that becomes saturated with the waste particles during polishing. This may result in false potential readings and may present a time lag because of the required pad flushing to

remove the waste particles. Since a fast and accurate endpoint detection method is required, this method is not feasible.

2.2.5 Optical Methods

There are many possible optical detection methods that measure the surface quality of the wafer. This section will discuss some of the key methods. For example, the interferometry technology measures the thickness of the ILD layer. The majority of the thickness measurement is done off-line and gives significant results to verify the performance of the polishing process. Another method, for example, measures the planarity of the ILD surface that indicates the endpoint [12]. For this, a light beam at a significant angle is emitted on the wafer surface. It detects the scattering effect, which gives an indication of the surface roughness. Once the sensor measures a decrease in scattering, the polishing process is stopped. Figure 2.9 shows these configurations.

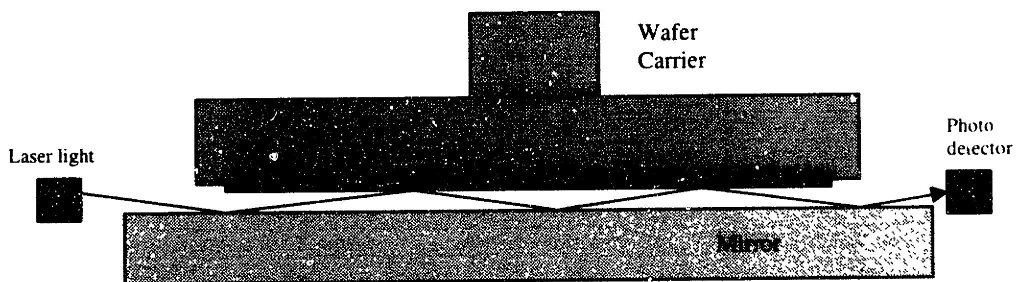

Figure 2.9 Optical Detection Setup (Scattering)

During metal polishing, the reflectance measured from the wafer surface indicates the presence of various materials. Initially, when only metal is present, reflected light intensity is high and remains constant. However, as the metal thickness approaches zero,

the reflectance signal changes noticeably as seen in Figure 2.10. This method will be discussed more in the following chapters.

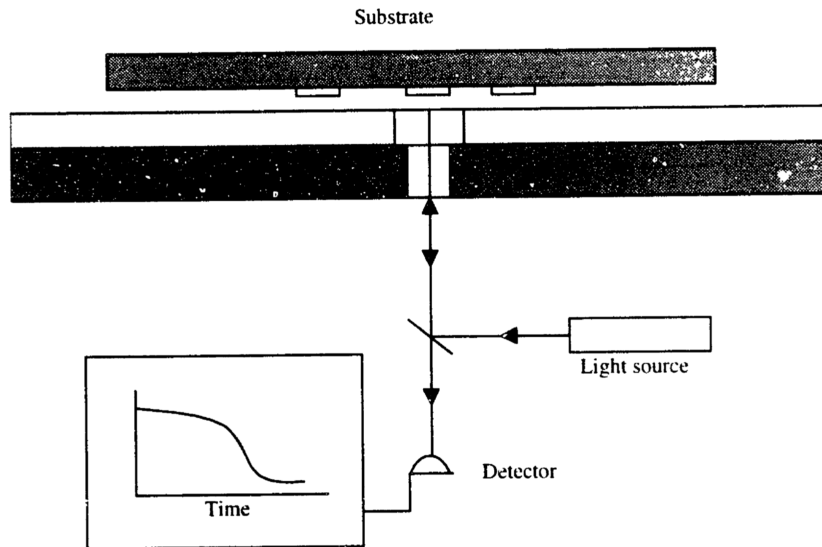

Figure 2.10 Optical Detection Setup (Reflectance)

Thermal images of the wafer surface while being polished can also indicate the endpoint. An infrared camera, slightly below or flush with the polishing pad, is able to measure the temperature of the wafer surface. The temperature change during polishing results from *friction by-product* or *chemically exothermic reactions*. The generated heat is a function of materials being polished, consumables, pad type, and the pattern density on the wafer.

All of the previous optical methods detect a single endpoint during polishing. However, the following method monitors the removal rate. Here, an x-ray beam is emitted on the slurry downstream of the wafer. The measured fluorescence and the removal rate depend on the density of the abrasives in the slurry. In principle this method can be used to determine the removal rates of ILD.

Most of the optical methods require viewing the wafer surface directly to measure the surface characteristics. Perhaps the simplest way to accomplish this is to overhang the wafer from the edge of the platen. This allows the sensor to have a clear view of the wafer. However, this method requires modifying the process parameters to move the wafer partially off the platen. Furthermore, the edge of the pad introduces transient effects that may cause non-uniformities on the wafer. Finally, with the wafer hung over the edge of the platen, the overall removal rate decreases and thus the polishing time increases. Another viewing scheme houses a sensor inside the wafer carrier and looks at the wafer from behind. The benefit of this setup is that the sensor always sees the wafer. However, it is only viable for one or two layers due to multi-layer interference. To alleviate the problems of the previous two methods, a third scheme was developed. A thru-hole in the platen allows the sensor to have a clear view of the front face of the wafer while polishing.

2.3 *Summary*

This chapter has covered a wide variety of detection methods that are either currently being used in production or are simply laboratory fantasies. It looks at the developing innovations and has given an indication of which methods are the most feasible. The mechanical detection method offers acceptable results in production equipment. However, the global detection method is unable to measure uniformity levels across the surface of the wafer. This information is vital when altering process parameters to improve the overall wafer uniformity. Therefore, an optical method capable of local detection is presented as the best solution.

Chapter 3: Modeling the Wafer Surface Reflectance

There are many possible ways to detect the endpoint of polishing wafers. The optical detection method was chosen because it satisfies the in-situ and local detection criterions. To investigate any endpoint detection method, it is necessary to understand the fundamental changes that occur to the wafer surface during polishing. This chapter will develop a simple model of the reflectance associated with these surface changes and identify the endpoint during polishing.

3.1 *Surface Evolution*

The surface topography resulting from the damascene process was introduced in Chapter 1. The intent of this section is to show how the surface evolves during CMP. Even though the polishing process is not completely understood, general trends that affect the reflectance measurement can be seen.

The surface evolution of blanket and patterned copper wafers is modeled in this section. The blanket wafer has a uniform and planar layer of copper on the substrate. The patterned wafers use the copper damascene process, resulting in a surface topography that follows the inlaid features. Density is the fraction of the surface covered by these inlaid copper features. Circuit designers generally attempt to achieve a nominal feature density of 30~50%.

There is very little change in surface characteristics during blanket wafer polishing. The copper layer is simply polished down until it reaches the oxide layer. However, during patterned wafer polishing, there are four stages where the surface characteristics are vastly different. In the beginning, the copper deposition coupled with the inlaid

trench structures leaves a surface that is high in surface topography. These features wear down during polishing until the process reaches the second stage, where the surface is flat with a uniform layer of copper, similar to blanket wafers. With more polishing, the third stage is reached and, the uniform copper layer disappears to reveal the inlaid structures. Finally, in the fourth stage, over-polishing results in dishing into the copper lines causing topography to form again. These occurrences will be discussed in the following sections.

3.1.1 Planarization Stage

Surface topography after copper deposition is highly dependent on the inlaid features and the deposition process. An ideal pattern of 50% copper density and line width of 0.5 μm is modeled. This structure may be best described by a sinusoidal wave. The trough of the sine wave is directly above the trench where the copper is filled while the crest lies above the land area as shown in the Figure 3.1. When the widths of the copper lines become large, the resulting surface topography may be better represented by a corrugated square structure also shown in Figure 3.1. An example of the surface topography after copper deposition is clearly visible in Figure 3.2, where an actual picture of a patterned copper wafer is shown. This wafer is four inches in diameter and has features that range from 0.5 – 100 μm line widths. The lighter areas in the picture show high levels of diffraction resulting from high feature densities.

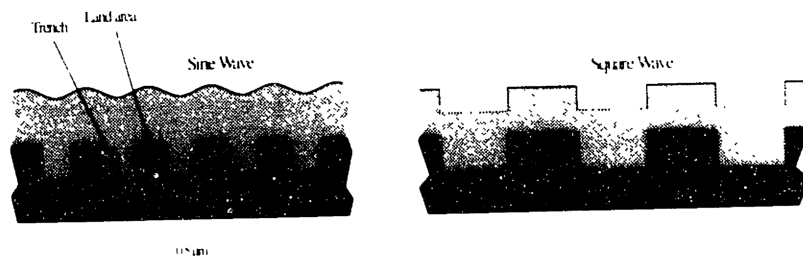

Figure 3.1 Wafer Surface Profile After Copper Deposition

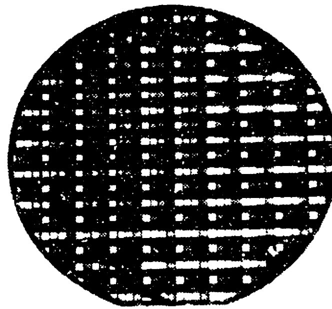

Figure 3.2 Picture of Patterned Wafer (Before Polishing)

During polishing, the amplitude of the sinusoidal wave decreases depending on the process conditions. For example, if the polishing pad is soft and conformal, it is more likely for the wave structure to be noticeable throughout polishing. However, if the pad is hard and rigid, only the high areas may be polished, resulting in the wave structure changing form.

3.1.2 Planar Surface Stage

This stage is the simplest to model. After polishing for a certain period of time, the high areas are worn down leaving a very planar surface, as seen in Figure 3.3. A picture of a polished wafer at this stage is shown in Figure 3.4. Notice that the topography seen in Figure 3.2 is much less evident after a period polishing, indicating that the surface is much more planar.

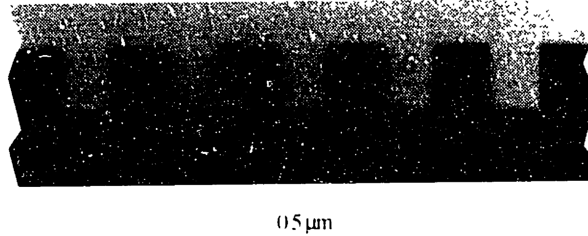

Figure 3.3 Wafer Surface After Planarization

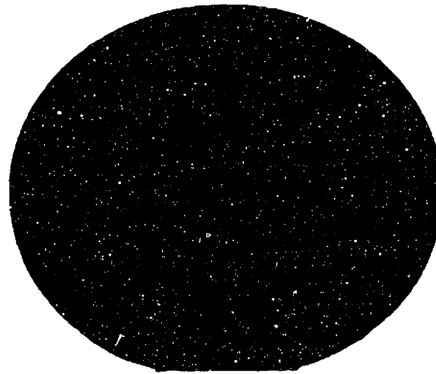

Figure 3.4 Picture of Patterned Wafer (Close to Planarity)

3.1.3 Metal Clearing Stage And Endpoint

As polishing continues, the copper layer becomes extremely thin and allows some light to penetrate through, and interact with, the inlaid features. Once, the copper layer is completely polished away, the surface becomes a combination of copper lines in the trenches and surrounding oxides. This stage shows very little dishing of the conducting lines and would be considered the optimal endpoint. The picture in Figure 3.6 shows a wafer at this stage. It exhibits high levels of diffraction due to the fine copper lines in the pattern.

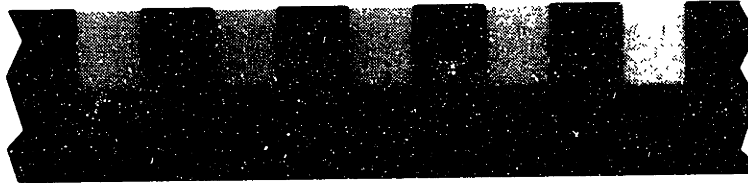

Figure 3.5 Wafer Surface at Endpoint

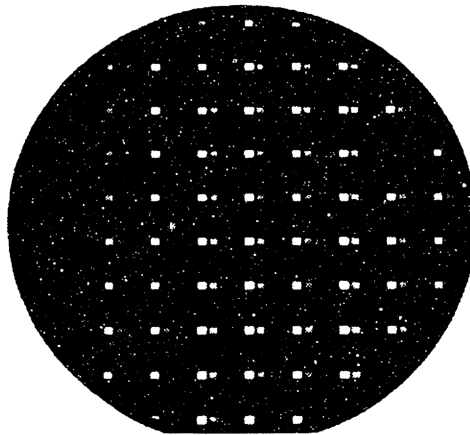

Figure 3.6 Picture of Patterned Wafer (At Endpoint)

3.1.4 Dishing Stage

This final stage shows dishing into the copper lines. The softer copper metal is polished more quickly than the harder insulating layer. Therefore, over-polishing of the wafer should be minimized, because dishing can limit circuit performance or scrap the wafer all together. It is likely that a sinusoidal surface profile will emerge again as seen in Figure 3.7.

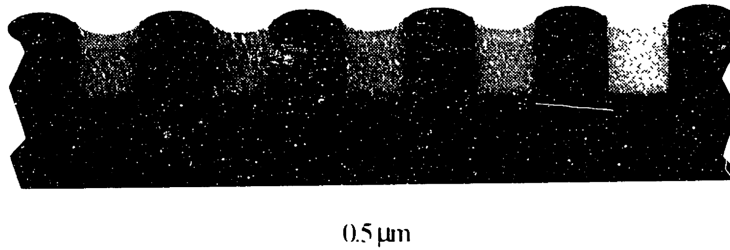

Figure 3.7 Wafer Surface with Over-polishing

3.2 ***Reflectance Characteristics***

Reflectance is defined as the fraction of incident light that is reflected by a surface. It is a function of material property, surface structure, angle of incident light, and polarization of light. During polishing, the first two factors change while the rest stays the same. This results in a detectable signal change that can indicate the endpoint. This section will associate reflectance values with the various surface conditions that were examined in the previous section.

3.2.1 Sinusoidal Surface

The reflectance from the idealized sinusoidal surface is analyzed in this section. However, it must be understood that the resulting surface topography can be vastly different, depending on the inlaid features. The sinusoidal surface profile is given by

$$\xi(x) = h \cos kx \tag{3.1}$$

where,

$K = 2\pi/\Lambda$

Λ= periodic wavelength

h= surface topography height

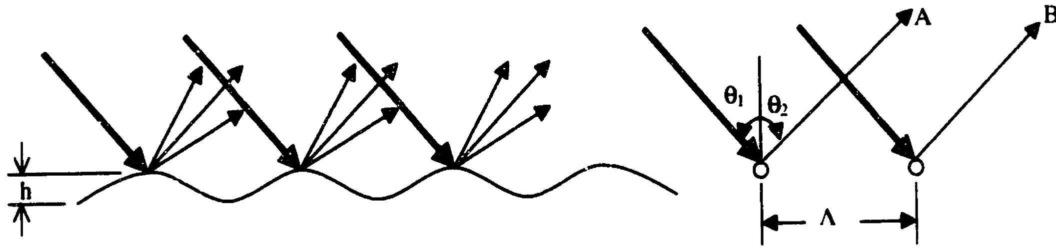

Figure 3.8 Sinusoidal Surface Structure

The reflectance from this surface is modeled by using diffraction theory. Hence, the overall reflectance is related by the scattering coefficient shown [13]:

$$\varphi = \frac{E_2}{E_{2o}} \tag{3.2}$$

Where,

E_{2o}= the field reflected in the direction of specular reflection ($\theta_2 = \theta_1$) by a smooth, perfectly conducting plane of the same dimensions under the same angle of incidence at the same distance, when the incident wave is horizontally polarized.

E_2 = measured reflected light.

The scattering coefficient (φ) can be calculated for this profile by:

$$\varphi^{\pm}(\theta_1,\theta_2) = \pm\frac{\sin 2np\pi}{2n\sin p\pi}\sec\theta_1\frac{1+\cos(\theta_1+\theta_2)}{\cos\theta_1+\cos\theta_2}e^{-ip\pi}\left[J_{-p}(s)+\frac{\sin p\pi}{\pi}\int_0^{\infty}e^{pt-s\sinh t}dt\right]+O\left(\frac{n_1}{n}\right) \tag{3.3}$$

where,

θ_1=angle of incident light

θ_2=angle of reflected light

$s= kh(\cos\theta_1+ \cos\theta_2)$

$$p = \frac{\Lambda}{\lambda}(\sin\theta_1 + \sin\theta_2)$$

$O(n_1/n)$= correction term

The reflectance from the wafer surface is calculated by using equation 3.2. It is the product of the scattering coefficient and the expected specular reflectance value. The scatter coefficient of a sinusoidal surface profile is calculated using equation 3.3. The scattering magnitude is dependent on the incident angle of light, the period of structure, the wavelength of light, and the height of the features.

The scattering coefficient is governed by the Bessel function, $J_0(s)$, when all of the necessary variables are inserted into the equation to solve for this case [14]. The scatter coefficient is a function of the surface height and periodic wavelength of the structure ($s=4\pi h/\Lambda$). To relate this coefficient with reflectance, the magnitude of the $J_0(s)$ is taken. The Figure 3.9 below shows how the scattering coefficient relates to surface topography. The height, h, is expected to be substantially smaller than the Λ, therefore, the region of interest is at the beginning of the Bessel function which is somewhat linear.

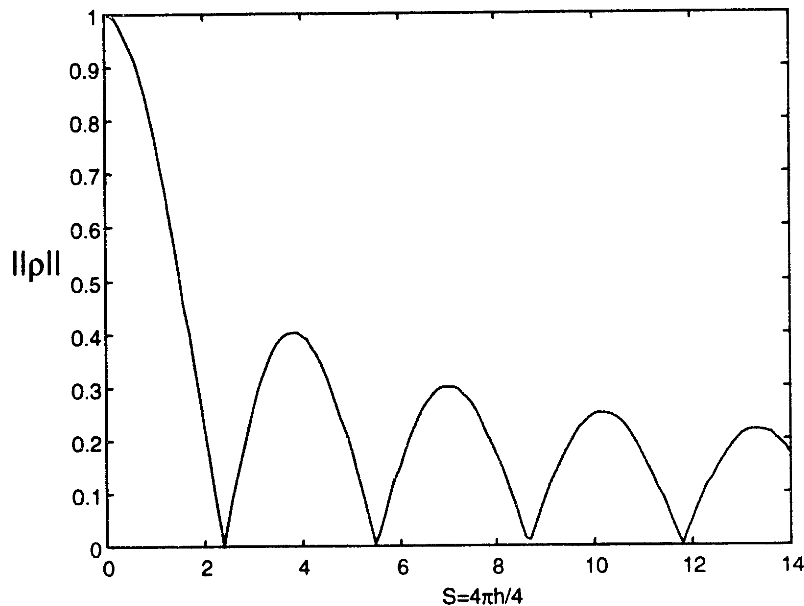

Figure 3.9 Magnitude Value of Bessel Function

3.2.2 Flat Surface

The topography will gradually decrease during polishing until the surface is void of noticeable features. At this time, the reflectance is mainly dependent on the material property of the wafer surface. The blanket wafer is always in this stage. It is modeled as specular reflection by a smooth and perfectly conducting planes as shown in Figure 3.10.

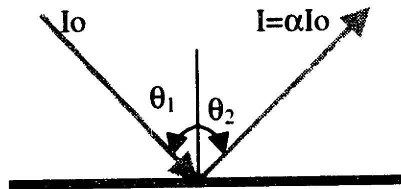

Figure 3.10 Specular Reflectance

3.2.3 Density Effect

The previous section shows the reflectance when the sensor measures only one type of material. However, when different materials are present, the overall reflectance is the sum of the individual product of reflectivity and density. The equation for overall reflectance is given by:

$$R = \rho_{Cu} R_{Cu} + \rho_{SiO2} R_{SiO2} \tag{3.4}$$

where

$\rho_{Cu} = A_{Cu} / A_{Total}$ = Copper density

A= area of the region

R= reflectance = I/I_o

3.2.4 Grating Surface

After the copper layer is polished away, the resulting surface consists of fine lines of copper surrounded by the less reflective oxide layer. This structure can be characterized as a grating system where close equidistant and parallel lines ruled on a polished surface, produce spectrum from diffraction. The grating characteristic is very important, because it appear at the endpoint of polishing. A simple model of this structure is a diffraction grating system, as seen in Figure 3.11. In case of the wafer, diffraction results from the thin copper lines reflecting back the light. Similarly, the diffraction grating system allows the light to pass through the slits causing similar diffraction effects. The reflectance from this type of surface may be best determined by empirical methods because of the variations that are present on a standard IC chip. The derivation of intensity for this type of reflection is beyond the scope of this thesis, yet general trends in intensity as a function of grating factors can be understood.

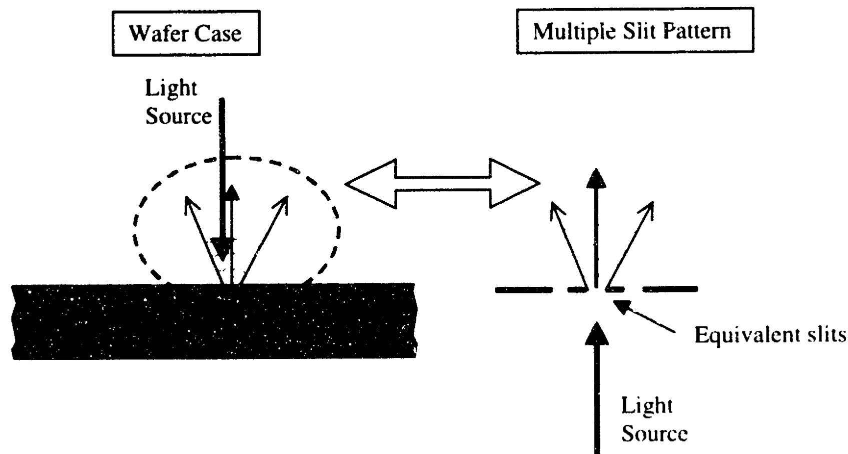

Figure 3.11 Equivalent Diffraction Configuration

The spatial distribution of the reflecting light from the Cu/Oxide composite surface can be described schematically by Figure 3.12. The central peak shows the maximum intensity, while the other peaks show lower intensity at specified angles.

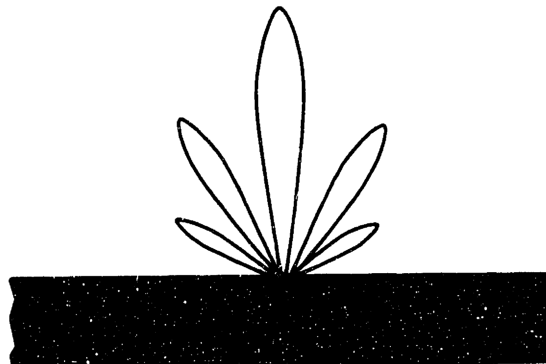

Figure 3.12 Diffraction Characteristics

3.2.5 Over-polished Wafer Surface

Dishing into the copper lines results in a lower reflective surface. This may be modeled by combining the sinusoidal profile effects with the grating effects. The Figure 3.13 shows a lower reflective surface due to the additional topography.

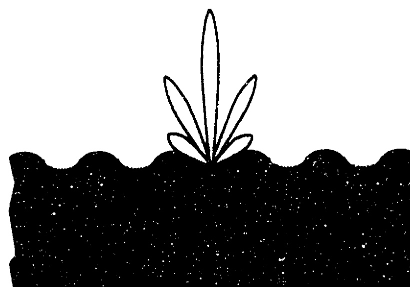

Figure 3.13 Diffraction from Rough Grated Surface

3.3 *Reflectance From Various Material*

In today's IC chips, copper and Si are some of the common materials used. The reflectivity of these materials is dependent on the wavelength of the light. Figure 3.14 shows handbook values of the reflectivity of various materials [15]. The reflectivity of metals is substantially higher than that of the Si. This fundamental difference in reflectivity is measured during polishing to determine the endpoint.

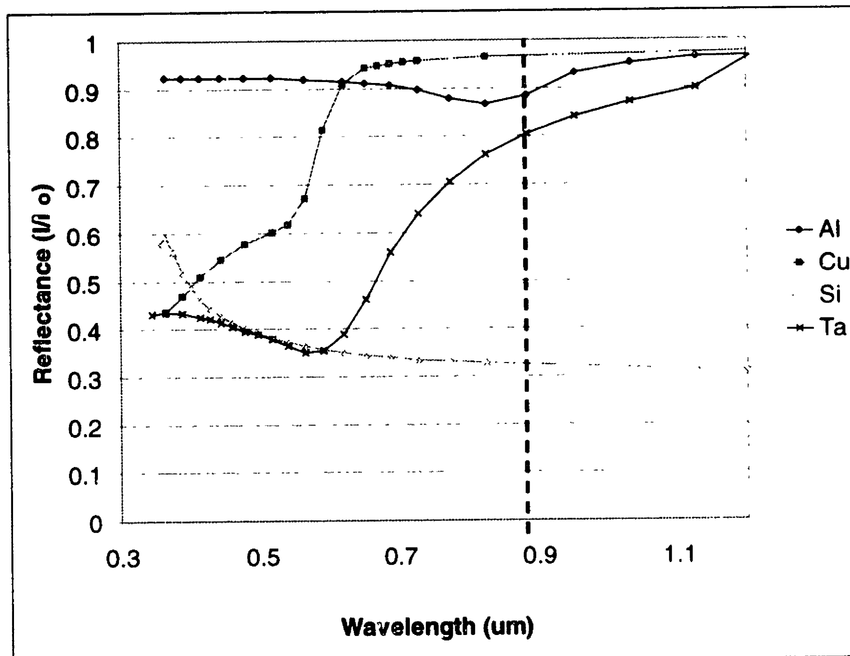

Figure 3.14 Reflectance Property of Common Materials

3.4 *Expected Reflectance Signal Trends*

3.4.1 Blanket Wafer Trends

As stated in section 3.1, during blanket wafer polishing, the signal does not change except at the endpoint. The uniform copper layer on the wafer surface is removed until the oxide layer is exposed. Figure 3.15 shows two plots, the ideal and the actual

reflectance trends. They represent what the sensor would measure when monitoring a specific region on the wafer while polishing. The difference in these plots can be attributed to the edge fast polishing and thinning of the copper film.

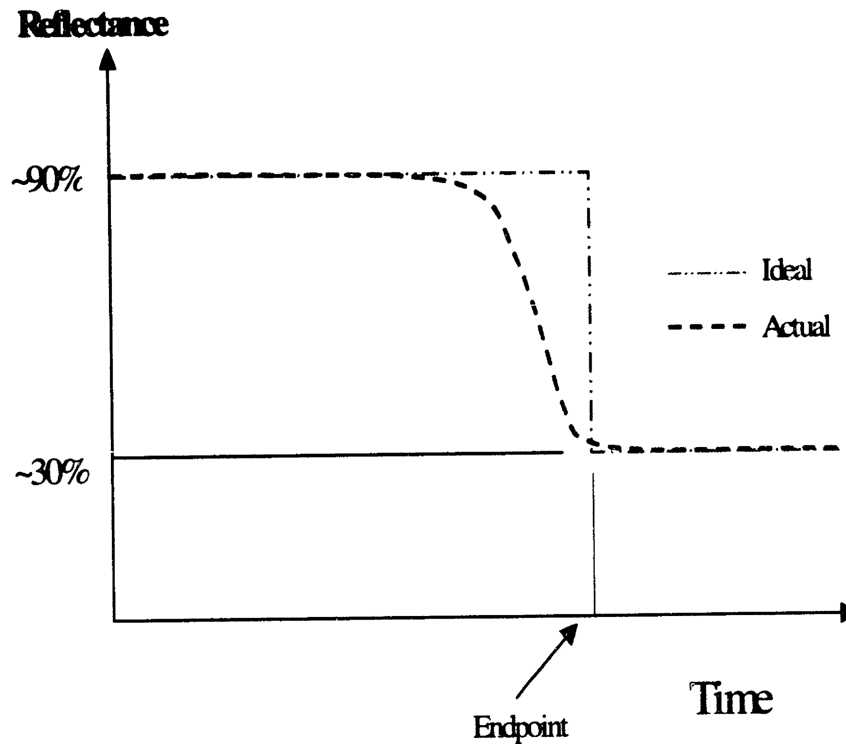

Figure 3.15 Reflectance Characteristics of a Blanket Wafer

3.4.2 Pattern wafer trends

Pattern wafers produce substantially different reflectance profiles when compared to blanket wafers, even though, the ideal trend shows very similar behavior. In the ideal model of 50% feature density, the expected reflectance at the endpoint is substantially higher than the blanket wafers due to the presence of copper as discussed in section 3.2.3.

However, the actual polishing trend in Figure 3.16 shows a very different profile from the ideal trend. It shows the four stages identified in section 3.2 as zones A, B, C, and D. The early polishing stage shows a reflectance that gradually increases. This is due to the

decrease in diffraction and scattering as the topography after copper deposition is planarized. After a certain polishing interval, the wafer surface becomes very flat and only specular reflectance is measured, resulting in a very flat signal. Thereafter, the signal decreases as copper is polished away from the land areas. However, the reflectance signal is much lower than the ideal trend due to the diffraction grating effects. The difference is noted as h_1. Finally, the reflectance further decreases, due to dishing, into the copper lines labeled as h2. The reflectance level (x) where optimal endpoint occurs depends on the pattern on the wafer surface. All of these trends can be seen in Figure 3.16.

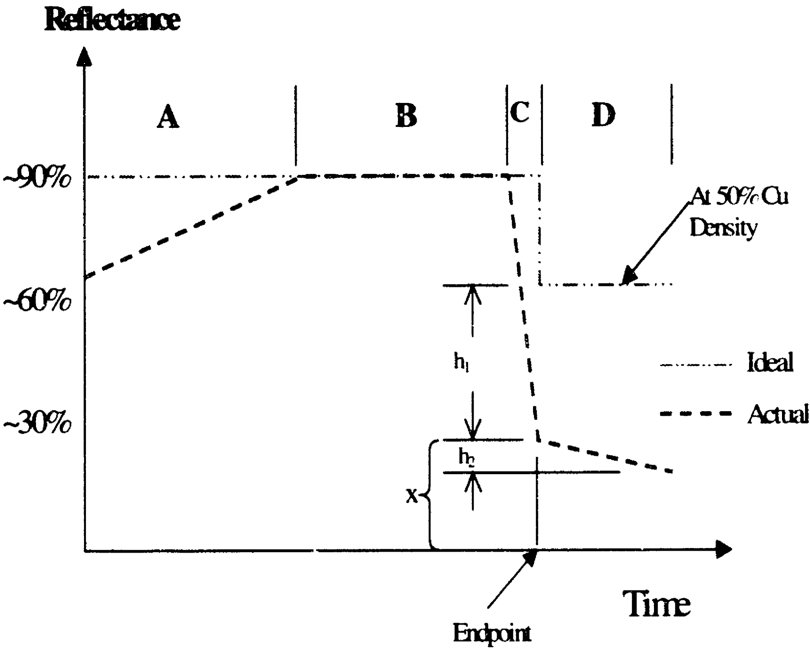

Figure 3.16 Reflectance Characteristics of a Patterned Wafer

Chapter 4: Design and Implementation

This chapter reviews the implementation of a reflectance sensor into a CMP machine. The sensor selection process and the design of the necessary supporting peripherals are discussed in this chapter.

4.1 *Sensor Requirements*

Many criterions were identified when deciding on which method to use for monitoring the polishing process. The most important is the ability to detect the wafer surface condition in-situ, or while polishing. The CMP process creates a harsh environment that is subject to change. Monitoring the process in-situ can account for many of these changes, and can result in a dynamic and accurate detection method. Another important requirement of the sensor is the local detection capability. The present CMP process can create edge fast polishing and other uniformity problems. Therefore, with local detection capability, polishing parameters may be controlled to improve the wafer level uniformity. Finally, the sensor should output a large signal change when the endpoint is reached.

4.2 *Sensor Choice*

After careful consideration of many possible detection schemes, the optical reflectance method was chosen. Thereafter, an appropriate reflectance sensor that met the requirements was found. The following sections review how the sensor was identified.

4.2.1 Axiomatic Design Decomposition

The axiomatic design methodology insures the uncoupled design of the sensor system. The functional requirements and the design parameters for this detection method are outlined here. There are two main requirements that need to be addressed: measuring the wafer surface conditions, and identifying when the endpoint occurs. The axiomatic decomposition is attached in Appendix A. This section focuses on the first requirement. the detection of the wafer surface condition.

4.2.2 Philtec Sensor

After the axiomatic design decomposition exercise, a reflectance sensor was chosen that met the above requirements. Furthermore, supporting structures were fabricated to accommodate the design parameters. The chosen sensor is a reflectance-dependent fiber optic displacement sensor made by Philtec.

In one application, the measured object is homogeneous and the gap between the object and the sensor is changed. This results in a signal that correlates the distance between the sensor tip and the specimen. In the reflectance detection mode. a constant gap is set and the material being measured is allowed to change. This results in an output signal that identifies the material's reflectivity. In this configuration, a light source with wavelength of 880nm is used, because it gives the greatest signal difference between the common metal and the insulating layer, copper and Si respectively, as is shown in Figure 3.14.

The sensor design is very compact with the amplifier measuring only 3"x 4" x 2". The optical fiber cable is 0.25" in diameter and 1ft long with a stainless steel tip. The tip is positioned at a specified distance from the object of interest. The 4.5" tip is specially

designed to meet the requirements of the sensor positioning system. The gap distance is selected to limit sensor output fluctuations when a slight variation in gap occurs. The sensor characteristics and the desired gap distance are seen in Figure 4.1.

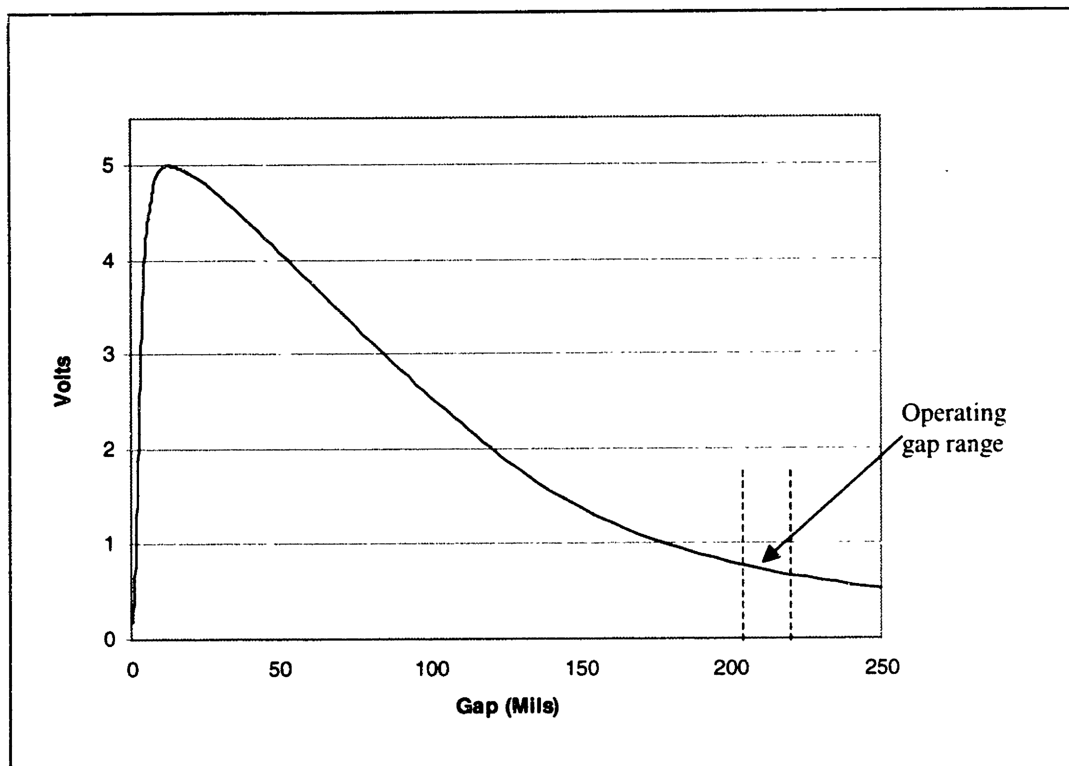

Figure 4.1 Philtec Sensor Characteristic

The sensor's internal component layout is shown in Figure 4.2. The high intensity LED emits the 880nm wavelength light on the surface of the specimen. The reflected light is measured by the photodiode, and the electrical components amplify and filter the signal. The system has low noise, and it is very sensitive to reflectivity changes.

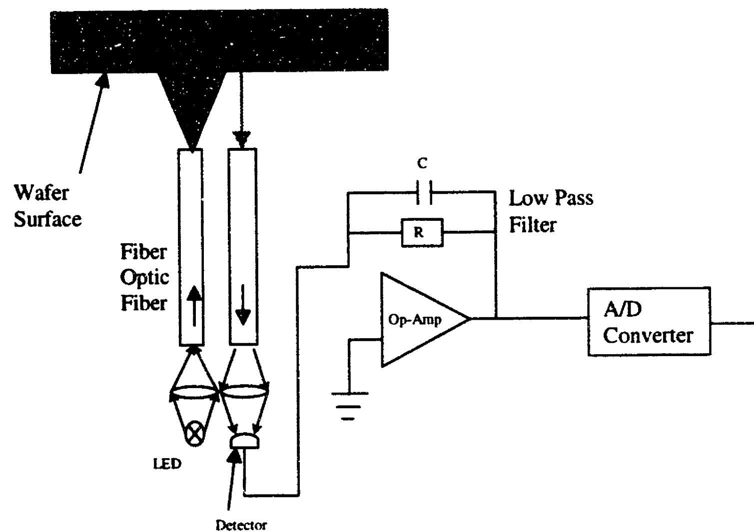

Figure 4.2 Sensor's Internal Components

Light Source	High Intensity LED, 880nm
Input Voltage	+9 to +30 VDC unregulated
Input Current	125ma max
Analog Output Voltage	0 to +5 VDC
Analog Output Current	5ma max
Frequency Response	DC to 20 kHz
Stability (electronic drift)	<5mv (i.e., <0.1% full scale)
Operating Temperature	0 TO 70° C
Weight	0.60 kg (1.3 lbs.)

Table 4.1 Philtec Sensor Specifications

4.3 *Implementation into the Alpha Machine*

The objective of this research was to develop a sensor that is incorporated into a newly designed CMP machine. Therefore, it was necessary to review the machine design and its history. The project was initiated three years ago with a company sponsorship. It consisted of four graduate students who designed and built the CMP machine. Other graduate students researched the process side of CMP on a test bed that was built two

years ago. Four professors of the mechanical engineering department were also involved in designing the machine.

4.3.1 Overall Machine Structure

The overall alpha machine design consists of three major structures. The lower structure, the upper structure and the wafer carrier assembly. This section will visit each of these structures and offer an explanation of their special features.

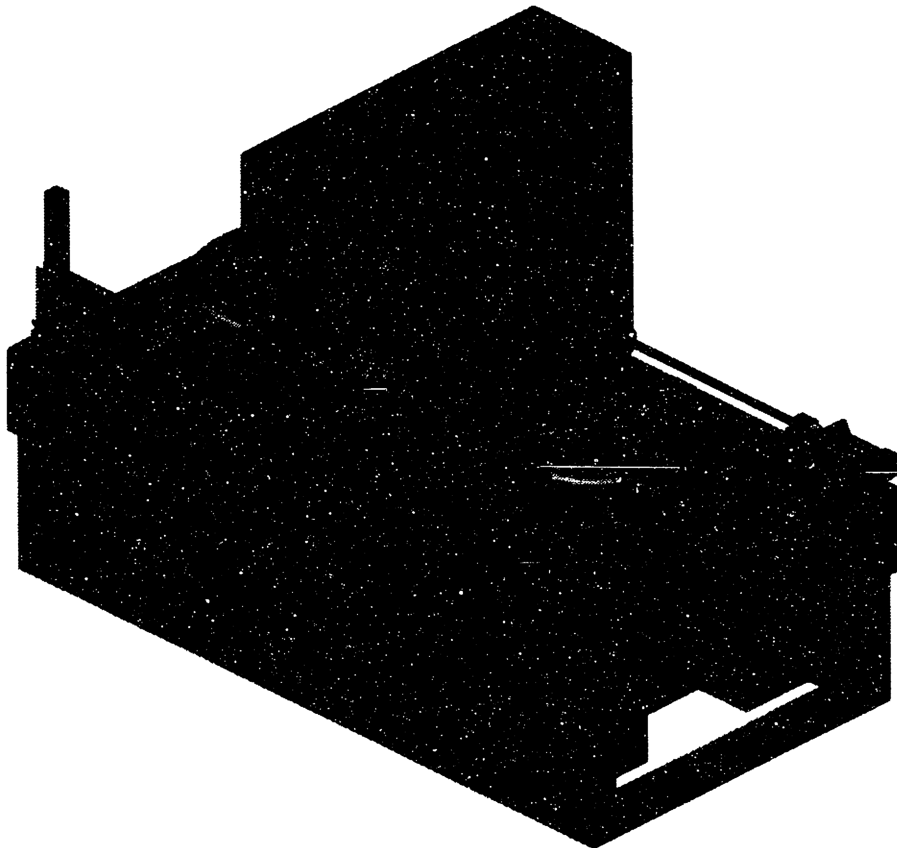

Figure 4.3 Alpha CMP Machine

Lower Structure

The lower structure consists of a large granite table measuring 108" long, 55"wide, and 12" thick, which is supported by a base made of welded hollow tubes. The flatness of

the table is 5 mils over the entire surface and is used as a datum to which other structures are referenced. This structure supports the upper structure as well as the wafer carrier assembly. These features can be seen in Figure 4.4.

The rotating platens and the load/unload station are assembled to this table. The polishing process is accomplished by applying velocity and pressure to the wafer by the platen and the wafer carrier. A super quiet motor, designed for the navy submarines, rotates the platen. This results in a smooth system with very low mechanical noise. Furthermore, the motor has a large bore that accommodates the slurry delivery and endpoint detection systems. Finally, a large diameter high precision bearing provides the support for platen rotation. It is located directly under the load exerted by the force application system. This eliminates the large, lever-arm effect that is found on comparable systems with the bearings on the spindle shaft.

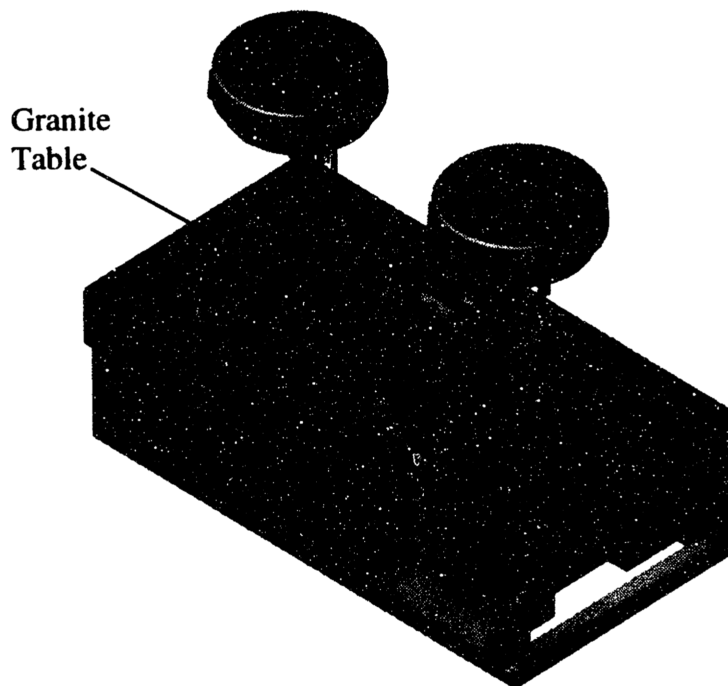

Figure 4.4 Granite Lower Structure

Upper Structure

The upper gantry structure is the force application system that is required for polishing. This assembly, which weighs over 2000 lbs, is made of welded hollow tubes that give it stiffness, yet minimize weight. The deflection experienced by the gantry is minimal and is only in the z-direction, without any induced moments. This structure slides on a pair of linear guides for the main x-axis motion and is actuated by ball screws. A pneumatic piston and a ball screw in parallel provide the vertical movement and force for the wafer carrier assembly. Similar to the x-axis, the carrier assembly is mounted on a pair of linear guides. The wafer carrier is dependent on the gantry for the x and z-axis motion.

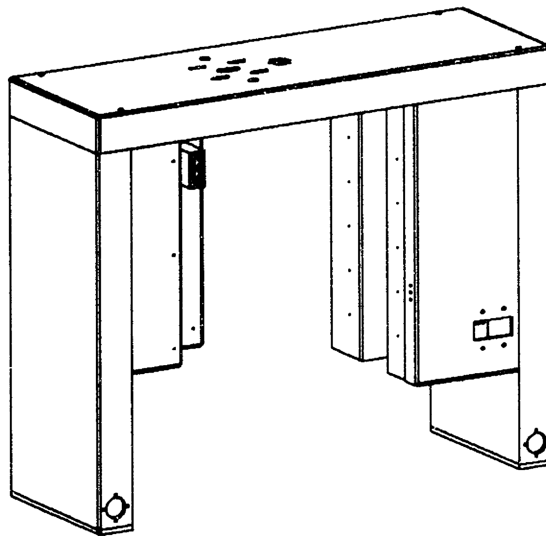

Figure 4.5 Gantry Upper Structure

Carrier Structure

The carrier assembly has the task of holding and applying a pressure profile to the backside of the wafer. The assembly boasts a series of bellows, which create the nominal pressure, while the individually controlled chambers, made of a segmented rubber

membrane, allow for fine controlling of the pressures. The wafer level uniformity may be controlled by a series of trial and error runs to converge on the optimal pressure profile. However, an alternative to this wasteful method is to measure the wafer's surface characteristic in-situ to determine the correct pressure profile. This unique feature may allow better wafer level uniformity control.

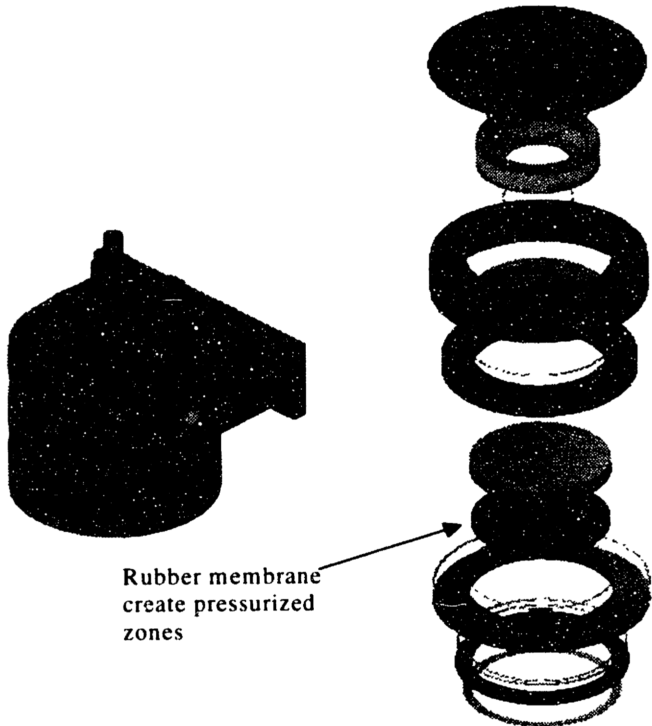

Figure 4.6 Carrier Assembly

4.3.2 Integration of Sensor into Platen

It is necessary to show an overview of the machine design to clarify how the in-situ sensor is integrated. The reflectance sensor is embedded in the platen and views the wafer through a ½ inch thru-hole. As the platen rotates, so do the sensor and the amplifier. Therefore, a rotary coupling is required to link the sensor to the power source and the data acquisition system. The mercury-filled coupling produces very little noise

and is able to transfer the sensitive reflectance signal without distortion. Couplings have two parts, the stator and the rotor. The rotor rotates with the platen and the sensor leads are attached to the contact terminals. Similarly, the stator is stationary relative to the machine. The power source and the data acquisition system attach to its contact terminals.

During polishing, the sensor needs protection from the environment, while still being allowed a clear view of the wafer. In particular, the slurry is abrasive and can cause damage or obstruct the view of the sensor. Rodel, a leading manufacturer of polishing pads and slurry, provides the window pad for polishing. A polyurethane pad holds a translucent window made from a material called JR111. This material is designed to have similar wear properties as the polishing pad, and will not protrude to damage the wafer when abrasives and conditioners wear the pad down. Figure 4.7 shows how all of these components come together.

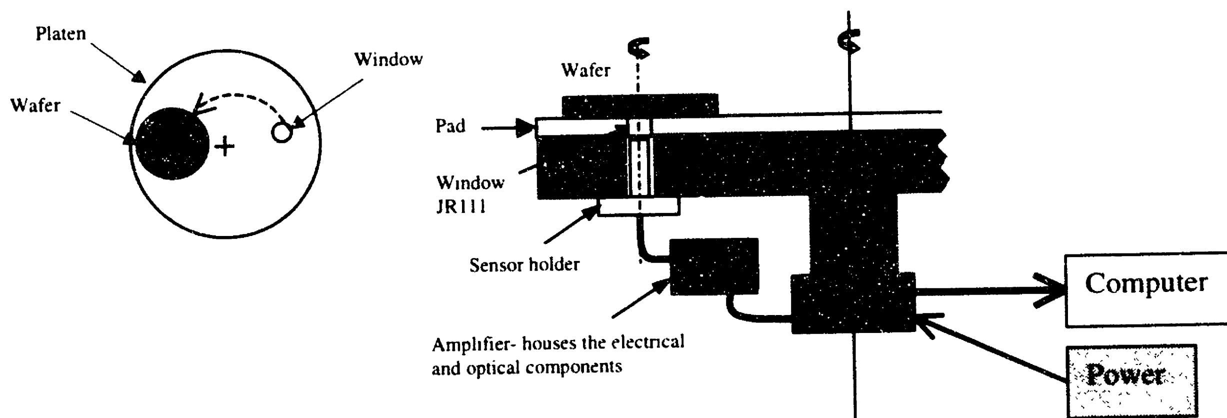

Figure 4.7 Sensor Implementation

4.3.3 Sensor Holder Design

Axiomatic decomposition reveals specific design parameters that need to be solved. Specifically the DP 151, mounting the sensor, is examined in this section. It requires a sensor holder to align and protect the sensor. The Philtec sensor from section 4.3.2 requires a view that is normal to the wafer's surface. This eliminates the need for complicated fixtures. However, the gap between the wafer and the sensor tip is critical for optimal detection. The fine vertical adjustment of the sensor tip is accomplished by the screw and nut configuration. The base of the sensor tip is treaded and the specially designed nut translates the sensor axially when rotated. The nut also holds the sensor securely when adjustment is not needed. The sensor holder constrains all degrees of freedom except axial movements, as seen in Figure 4.8.

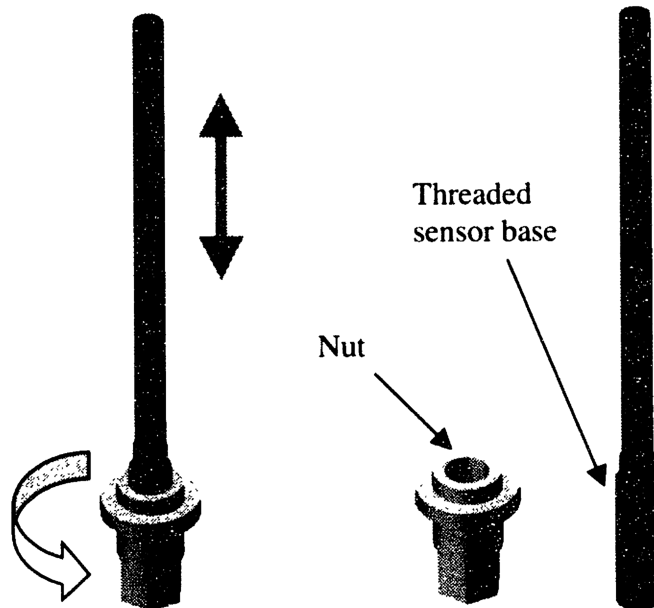

Figure 4.8 Vertical Adjustment Mechanism

The holder protects the sensor from the environment in two ways. Slurry is kept away from the sensor by sealing the tip of the holder with a fused silica window. In addition, the stainless steel housing protects the sensor tip from impacts during assembly of the system. The holder is attached to the platen by a semi circular flange. This design is necessary to allow the holder to be positioned closer to the spindle walls without interference. This gives the sensor the necessary offset from the platen center without affecting the spindle design. A detailed drawing of the sensor holder is attached in Appendix B.

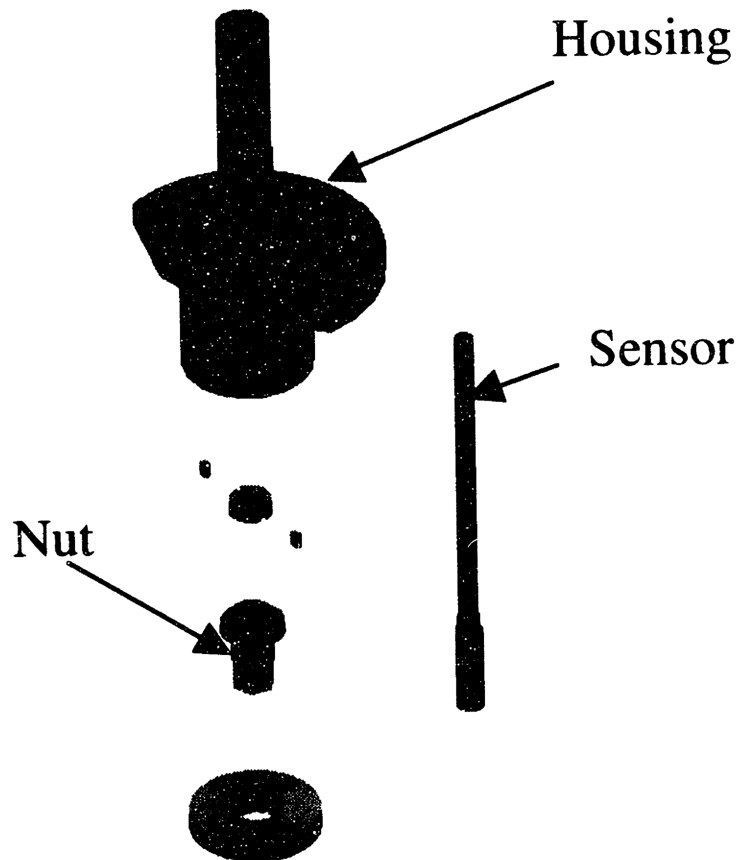

Figure 4.9 Sensor Housing

4.4 *System Kinematics*

It is important to understand the kinematics of the machine and its effects on the output signal of the sensor. The section that covers the overall machine design shows a system that contains two platens and a wafer carrier. The wafer carrier is able to move between the two platens depending on the process demands. This section will discuss the velocity distribution across the wafer surface, as well as the sensor position relative to the moving wafer during polishing.

4.4.1 Velocity Distribution

When the angular speed of the platen and the wafer carrier are the same, the velocity distribution across the polishing interface is uniform. The magnitude of the relative velocity is the product of the platen's angular velocity and the center to center offset between the wafer and platen.

4.4.2 Sensor Position on the Wafer

Applying the coordinate transformation to the rotating bodies, a position of the sensor relative to the wafer can be found. This may be advantageous so that an expected signal can be developed. The following equations calculate the sensor location:

$$x = d\cos\theta_w + r\cos(\theta_w + \theta_p) \tag{4.1}$$

$$y = d\sin\theta_w + r\sin(\theta_w + \theta_p) \tag{4.2}$$

where

d= wafer center to platen center offset

r= sensor offset

θ_w= rotation of the wafer

θ_p= rotation of the platen

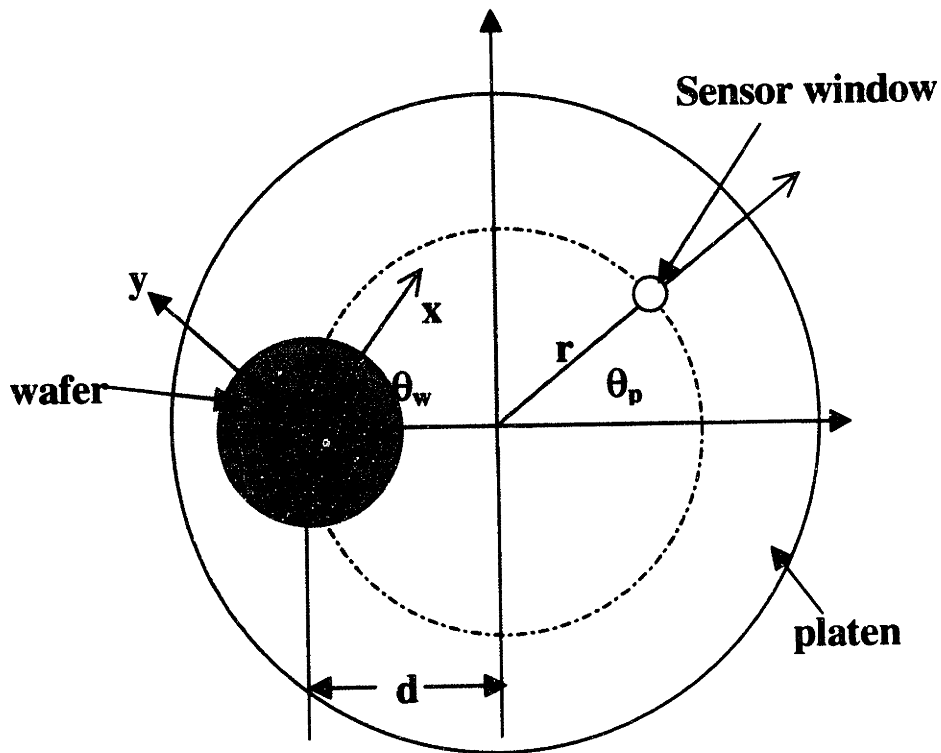

Figure 4.10 Coordinate System of the Rotary Configuration

4.5 *Sensor Validation*

Originally, plans were scheduled to test the optical detection method in the Alpha machine. However, schedule setbacks during the machine design phase ultimately made these plans impossible. Therefore, the test bed was modified to accept the sensor. This allowed the testing of the sensor in an actual polishing environment.

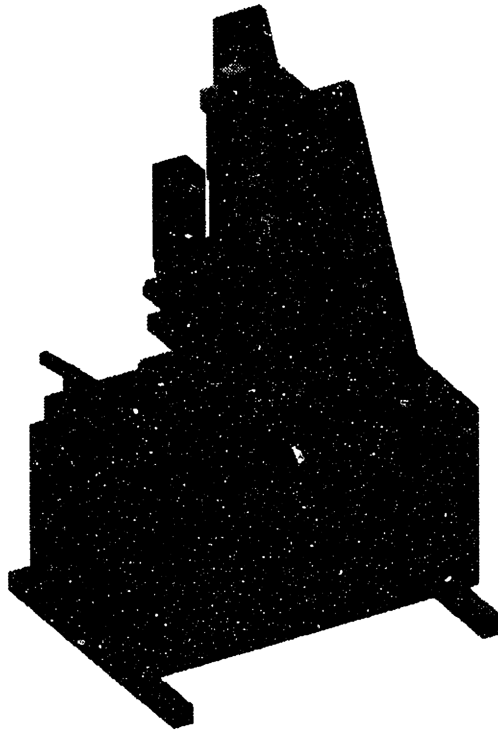

Figure 4.11 Test Bed Polishing Machine

4.5.1 Problems with the Test Bed Implementation

The original test bed design has made it impossible to implement the sensor. First, the spacing below the platen was inadequate and had to be lengthened. This was accomplished by designing a shaft extender to lengthen the shaft by 4 inches, which allowed enough room for the sensor holder and the amplifier. Furthermore, the splashguard was redesigned to fit the new configuration. To simplify and accelerate the design and fabrication of the guard, it was made from pieces of 1/8-inch thick low-density polyethylene plastic. Finally, the platen was modified to hold the sensor, as well as the amplifier.

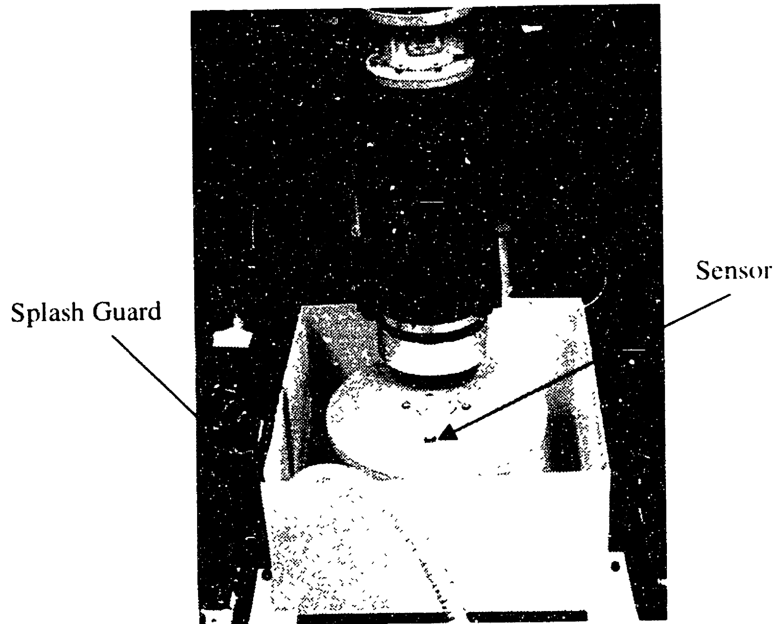

Figure 4.12 Test Bed Modification

4.5.2 Differences Between the Alpha Machine and Test Bed

The greatest difference between the test bed and the alpha machine is the spindle design. A solid 1.5-inch shaft supports the platen on the test bed while the alpha machine is designed with an 11.5-inch hollow spindle. It is expected that the alpha machine will have superior performance as compared to the test bed, and will also result in less noise in the environment

4.5.3 Similarities Between the Alpha Machine and Test Bed

The rest of the design between the alpha machine and the test bed is very similar, especially the power and signal transfer mechanism. The test bed transfers the necessary elements through a slip ring while the alpha machine sends its elements through a mercury-filled rotary coupling. The coupling used in the alpha machine should out perform the slip ring by creating less noise in the output signal.

Chapter 5: Experimental Results

This chapter presents various experiments that have helped to explain and test the reflectance endpoint detection method. Simple experiments, ranging from sensor performance tests to in-situ measurements of wafers being polished in real time, were performed to verify the reflectance method.

5.1 *Sensor performance*

5.1.1 Material Property Testing

One of the most basic experiments involved measuring the reflectance of materials that are commonly used in the design of IC chips. The reflectance values were then compared to the theoretical handbook values shown in section 3.3. The setup for the experiment consisted of a bench designed to provide a reference plane for the wafer to sit on, while its reflectance was being measured. This design provided a repeatable gap between the wafer and the sensor tip, as shown in Figure 5.1. The sensor was positioned under the bench, and looking up at the wafer, similar to the alpha machine. Table 5.1 compares the theoretical (handbook) values to the measured values of copper, aluminum, and silicon. The measured values are very similar to the theoretical values, however, slight differences in their magnitude is evident. This is due to roughness of the surface and variations in the purity of the materials.

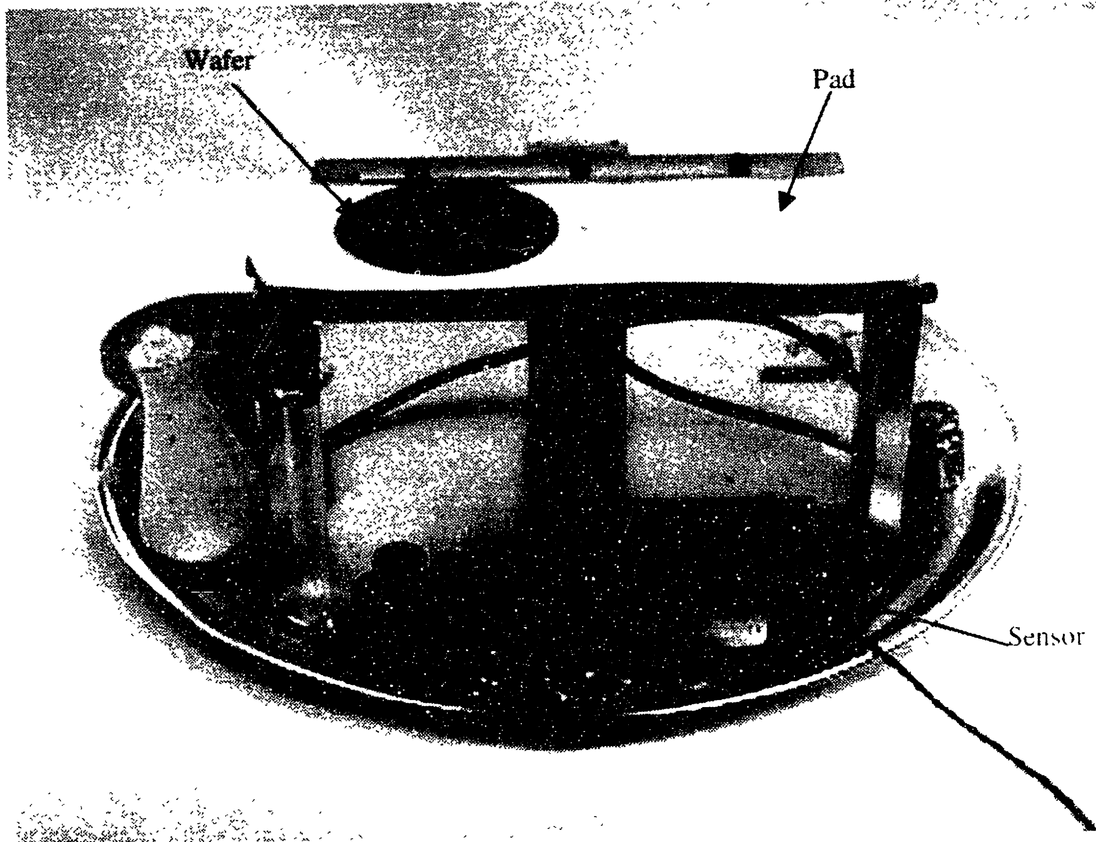

Figure 5.1 Test Bench Setup

	Handbook	Measured
Cu	97 %	97%
Al	89%	86%
Si	32%	28%

Table 5.1 Reflectance of Various Material

5.1.2 Effects of Slurry

This experiment measures the reflectance of a copper wafer when slurry at the polishing interface obstructs the penetration of light. Slurry is a mixture of transport/lubrication liquid with abrasive particles that are generally less than 3 microns. The intensity of the reflected light decreases as the thickness of slurry in the polishing interface increases.

The existing CMP test bed is modified to measure these effects. This simple modification is made prior to the one discussed in Chapter 4, and the resulting kinematic system is very different. Nonetheless, this new system provides the necessary relative velocity and pressure that is required to measure the effects of the slurry and the window in an environment similar to that of the actual CMP machine.

Prior to this modification, the wafer and the polishing pad both rotated to create a uniform relative velocity, while the sensor viewed the wafer through the platen. However, in the new system, the wafer carrier assembly is no longer used to rotate the wafer. Rather, the carrier assembly is stationary, holding the sensor and a small piece of polishing pad from above. A small window is imbedded in the polishing pad so that the sensor may have a clear view of the wafer. This assembly provides the vertical force that is required to remove material during polishing. The other essential component for polishing is velocity, which is provided by attaching the back of the wafer to the rotating platen, as shown in Figure 5.2. However, since the head is now stationary, this system creates a velocity distribution across the polishing interface that results in a non-uniform removal of the copper layer. Another difference is the surface area of the pad available for polishing the wafer. The new system has substantially smaller area than an actual

polishing machine. This results in a much slower removal rate of the wafer surface materials.

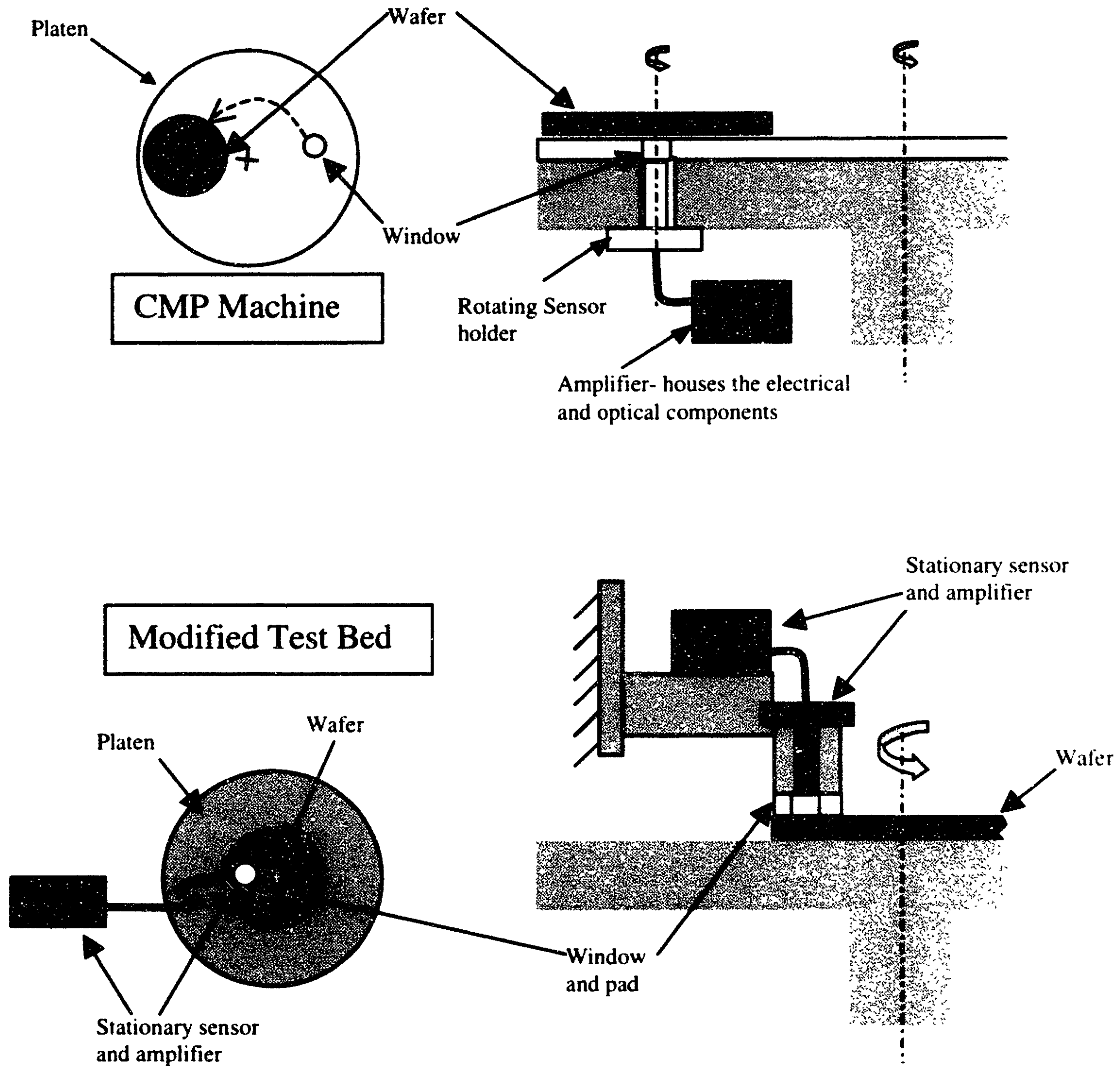

Figure 5.2 Test Bed Modification

The new test bed setup uses flexible foam to provide the necessary gimbling of the polishing pad, keeping it parallel with the wafer surface. This is designed to prevent high pressure points. However, the gimble mechanism is not very effective in preventing

pressure distribution in the wafer-pad interface, which can also result in non-uniform removal rates.

Even though this setup proves to be insufficient in measuring the actual polishing characteristics, it successfully shows the effects of the slurry and the window in the CMP environment. The results show that the polishing action minimizes the slurry film thickness between the wafer and pad interface. It appears that the edges of the pad wipe away the excess slurry before it can enter and obstruct the reflectance measurement. The interference caused by the slurry and the window reduces the sensor's ability to detect the wafer surface, however, the effects are constant and small. The measured interference from the window and the slurry cause a 22% and 18% reduction in signal level, respectively.

5.2 *Incremental Reflectance from Patterned Wafers*

This experiment measures the reflectance from eight four-inch patterned copper wafers after being polished at increasing time intervals. These wafers contain 10x10 mm dies that are composed of 12 subdie areas, which are 2x2 mm in dimension. These subdies hold arrays of line structures that range from 0.5- 100 μm line widths, and densities that range from 0 to 50%. The reflectance values measured from a patterned wafer with a 0.5-micron and 50% density features are given in Figure 5.3. This figure resembles the polishing trends of patterned wafers modeled in section 3.4.2.

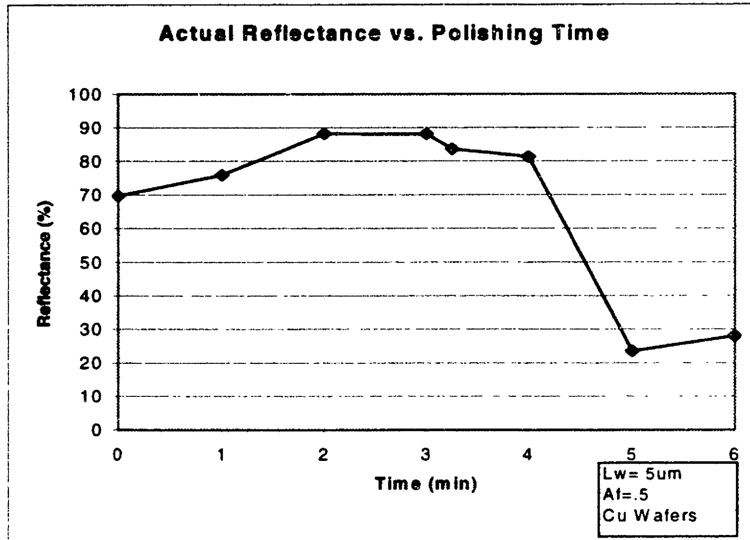

Figure 5.3 Reflectance of 0.5 μm Lines at 50% Density

5.3 *Test Bed Polishing Data*

In this section, blanket and patterned wafers are polished in a CMP machine as the final test of the optical sensor. The objective of this experiment is to collect data as the wafer is being polished. This data is compared to the theoretical models developed in chapter 3.

5.3.1 Experimental Parameters

The test bed modification required for this experiment was discussed in chapter four. The following parameters are used for polishing the wafer: a pressure of 7 psi. and a relative velocity of 0.7 m/s. The data acquisition system collects the data from the sensor at 1 kHz, which is sufficient to measure the reflectance over the entire wafer diameter each time the wafer passes the sensor.

5.3.2 Experimental Data

The total polishing time is about 3-5 minutes, depending on the desired over-polishing. During this time, the sensor views the wafer surface periodically and measures its reflectance. Figure 5.4 shows the average reflectance values across the wafer for a blanket wafer. The reflectance curve has a well-defined, repeatable trend. It is initially at 90% reflectance, which represents pure copper on the wafer surface. After polishing for a while, the copper layer is polished away, exposing the barrier layer, and then the Si substrate. This signal does not exactly follow the ideal trend since edge-fast polishing results in a more gradual change in the signal. However, there is a defined transition point when all of the copper is polished away and the barrier layer is exposed. The second transition point represents the barrier layer clearing, exposing the lesser reflective Si substrate.

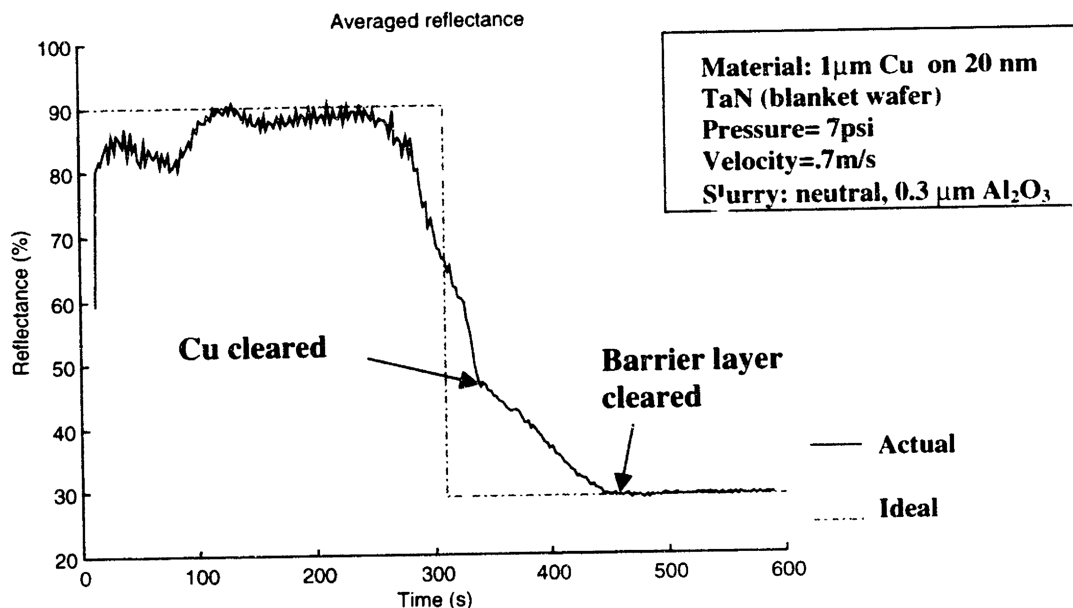

Figure 5.4 Blanket Wafer Polishing (Averaged Over Wafer)

The *averaged* reflectance in Figure 5.4 does not show the non-uniform clearing of the copper layer during polishing. Figure 5.5, shows a plot of the individual reflectance values measured across the wafer. Edge fast polishing and other non-uniformities are clearly visible in this figure. The three distinct reflectance levels of Cu, TaN, and Si substrate can be identified from the plot. Note that reflectance does not indicate the material thickness; it only indicates the presence of a material type.

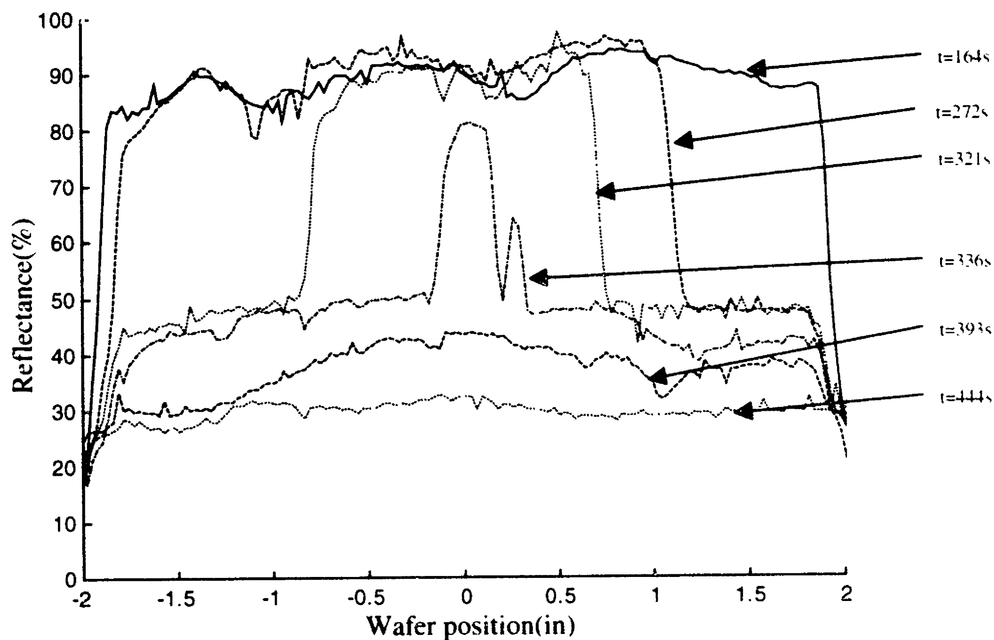

Figure 5.5 Blanket Wafer Polishing (Scanned Over Wafer)

5.3.3 Comparing the Wafer Surface Condition with the Sensor Reading

The figure shown in the previous section suggests that the center of the wafer is polished last. The sensor output is confirmed by polishing a wafer halfway through, until only a fraction of the copper is left on the surface. This way the sensor output and the wafer surface can be compared. Figure 5.6 shows the sensor readings and the corresponding wafer surfaces. This sensor reading agrees with the surface characteristics

of the wafers. The left picture shows the lighter, copper area polishing faster at the center. The corresponding signal shows similar reflectance characteristics. Similarly, the right picture shows the edge of the wafer polishing faster, and the sensor reading corresponds to this observation as well.

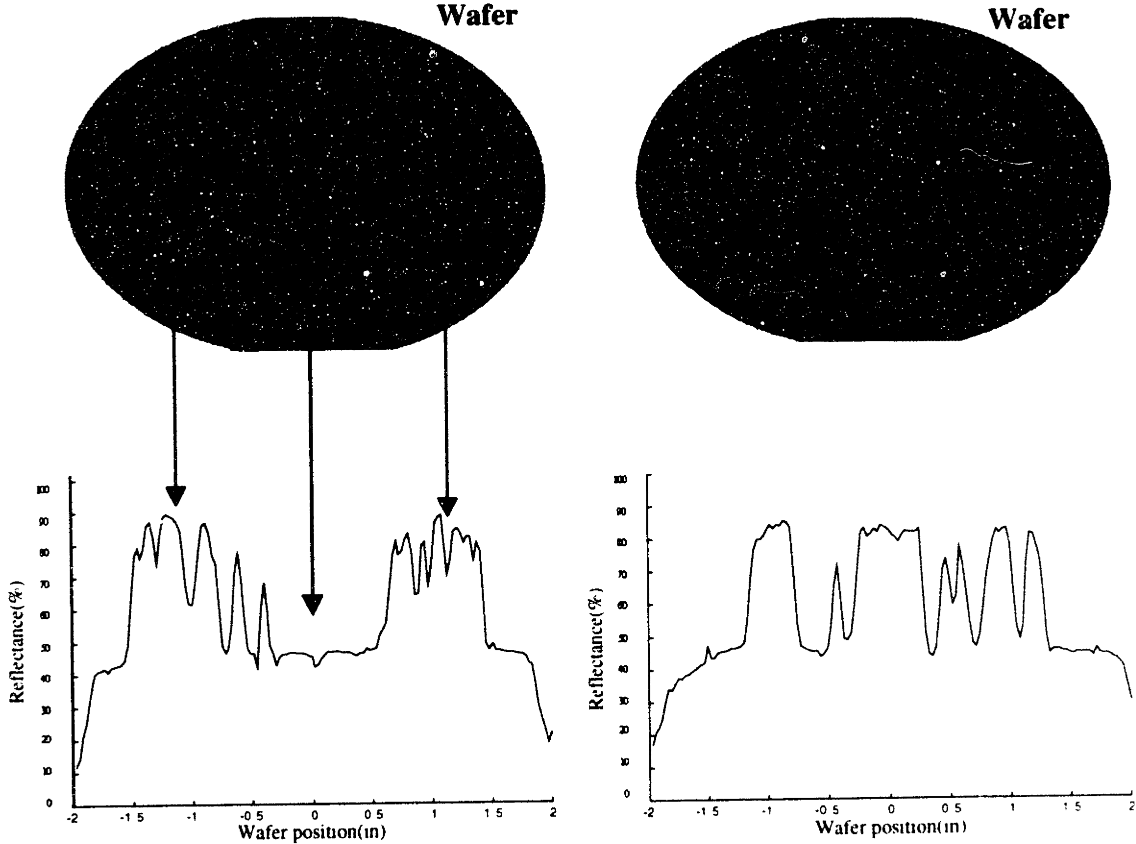

Figure 5.6 Correlation Between Sensor Signal and Physical Wafer Characteristics

5.3.4 Sensor Repeatability

Figure 5.4 shows the plot of polishing a wafer with a clear transition between the different materials on the surface. The purpose of this experiment is to determine the repeatability of measuring the changes during polishing. Figure 5.7 shows the results of polishing four blanket wafers. The slopes during the copper clearing stage are all very similar. Furthermore, the reflectance value at which all of the copper is cleared, leaving only the barrier layer, is very repeatable, as seen in Figure 5.7.

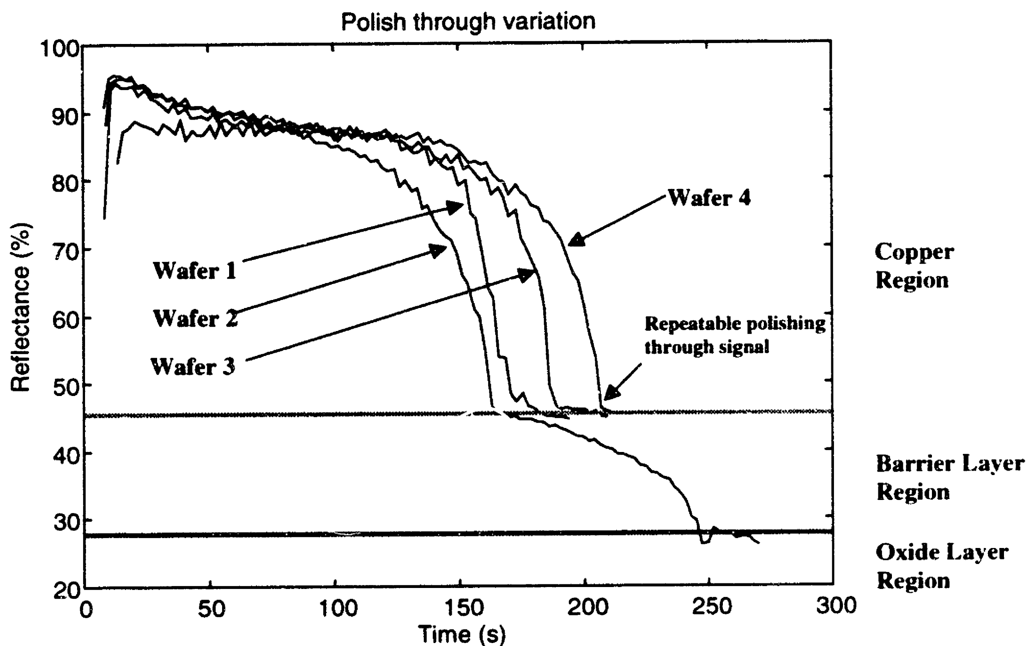

Figure 5.7 Multiple Blanket Wafer Polishing Results

5.3.5 Pattern wafer result

Figure 5.8 shows the polishing result for patterned wafers. The wafer in this experiment has the same design as discussed in section 5.2. The clear transitions seen during blanket wafer polishing are not as evident for this case. The gradual change in

reflectance originates from the trench structures affecting the polishing rates, as well as the overall reflectance characteristics. The averaged reflectance trend follows the patterned wafer polishing trend developed in section 3.4.2. The reflectance increases to a constant value once the surface has planarized. Thereafter, diffraction from grating structures and copper line dishing reduce the reflectance from the wafer surface.

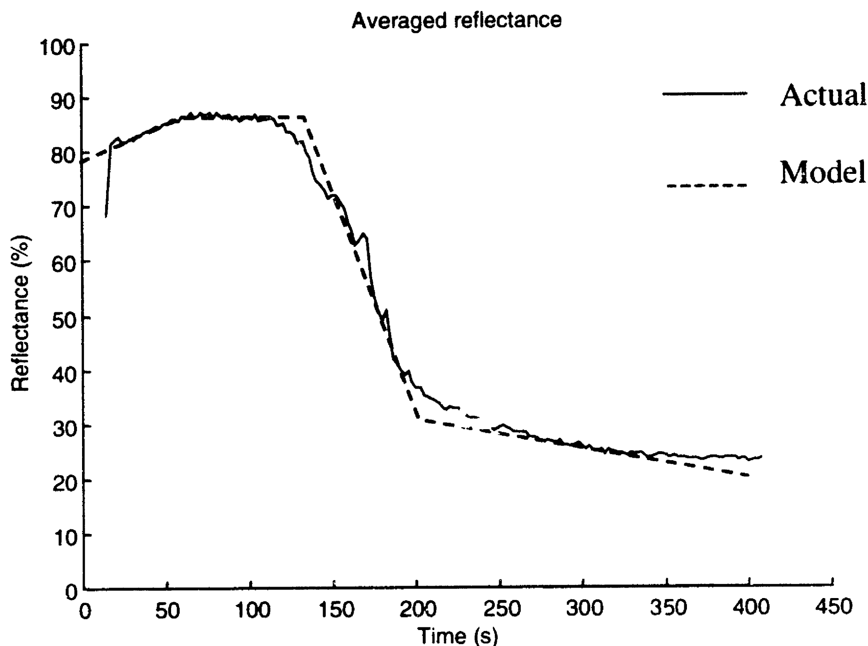

Figure 5.8 Pattern Wafer Polishing Results

5.4 *Signal Endpoint Characteristics*

While analyzing the data collected by the sensor, it is important to focus on certain characteristics that may indicate the endpoint. This task is not trivial, especially when *patterned* wafers are examined. The gradual change of the output signal makes it difficult to identify the exact time when optimal polishing has occurred. However, a simple analysis of the measured reflectance signal has revealed possible endpoint characteristics. The following sections will discuss these findings.

5.4.1 Threshold Comparison

In this detection scheme, the averaged signal level across the wafer is compared to a predetermined threshold value. This threshold value may be best determined by measuring multiple wafers during actual polishing. The endpoint has been reached when the measured signal becomes less than the threshold value. Polishing can then be stopped, or allowed to continue for a period of over-polishing to ensure that all the land area is clear of metals.

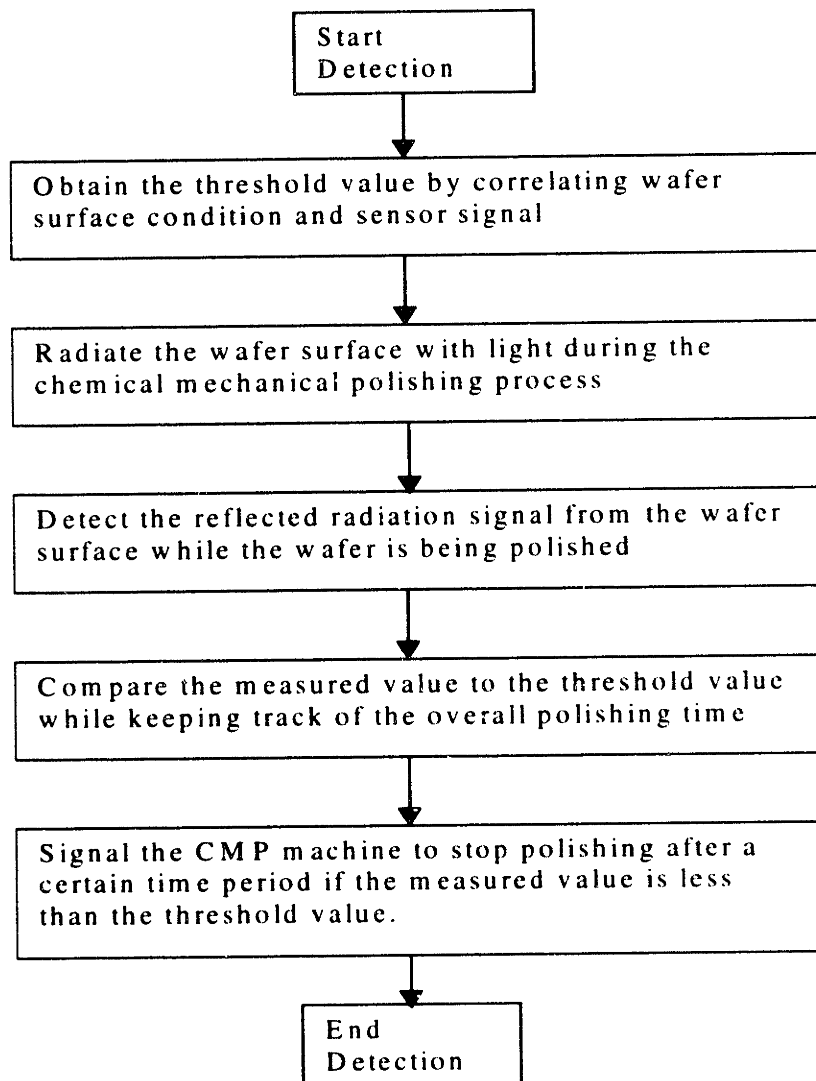

Figure 5.9 Threshold Detection Flow Chart

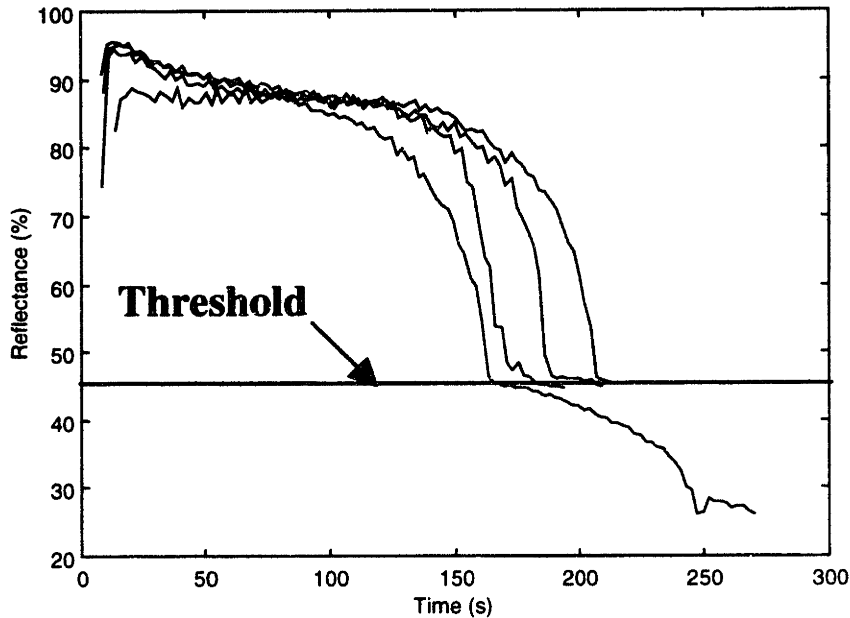

Figure 5.10 Threshold Comparison

5.4.2 Monitoring the Reflectance Change

For this detection scheme, the averaged signal is compared to the previously measured reflectance value. The rate at which the averaged signal decreases may give an indication of the endpoint. When there is a high rate of change, it is most likely the copper layer polishing through exposing the less reflective oxide layer. When the endpoint is approached, the rate of change decreases. Figure 5.11 shows the measured reflectance data from the sensor as well as the calculated rate of change in the signal. The two plots have different y-axes. The left axis shows reflectance values of the sensor data and the right axis gives the rate of change in the reflectance values. There are distinct characteristics in the rate of change plot that may be used for an endpoint indicator.

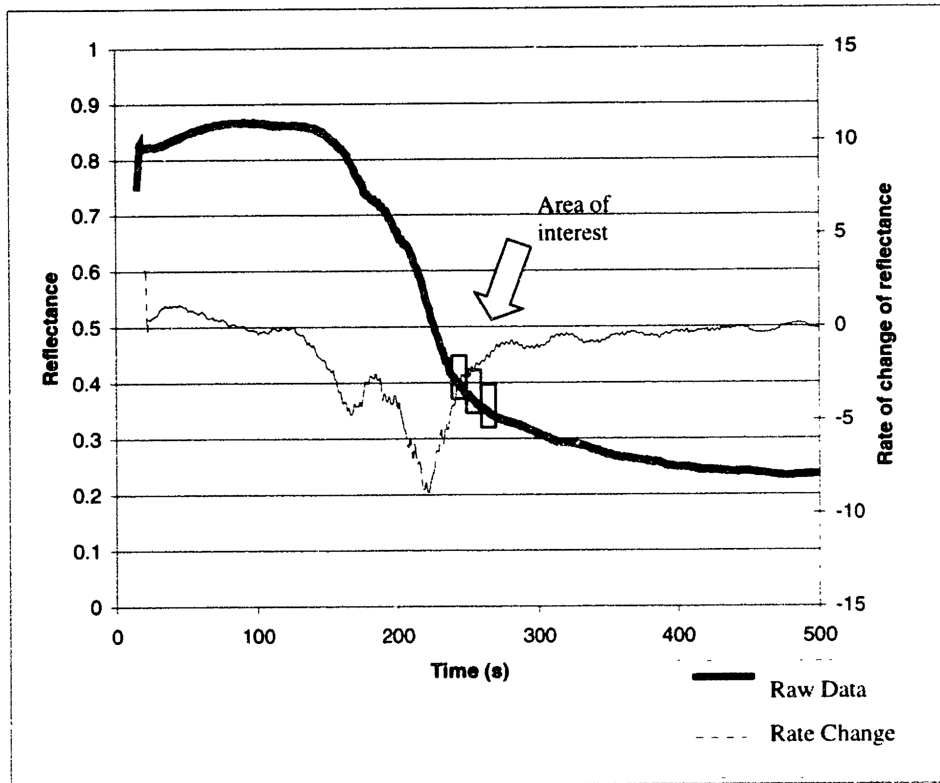

Figure 5.11 Change in Signal Detection

The detection may be done over the entire wafer as indicated above. However, the wafer may also be divided into zones of concentric rings to evaluate the polishing uniformity level.

5.4.3 Monitoring the Standard Deviation

This detection scheme relies on monitoring the signal fluctuations during polishing. As copper is polished away, the standard deviation of the measured signal increases, due to the large difference in reflectance of Cu and Si. However, when the majority of the copper layer is polished away, leaving only a pattern of copper lines, the deviation in signal drastically decreases. This change may be another indicator of the endpoint, as seen in Figure 5.12.

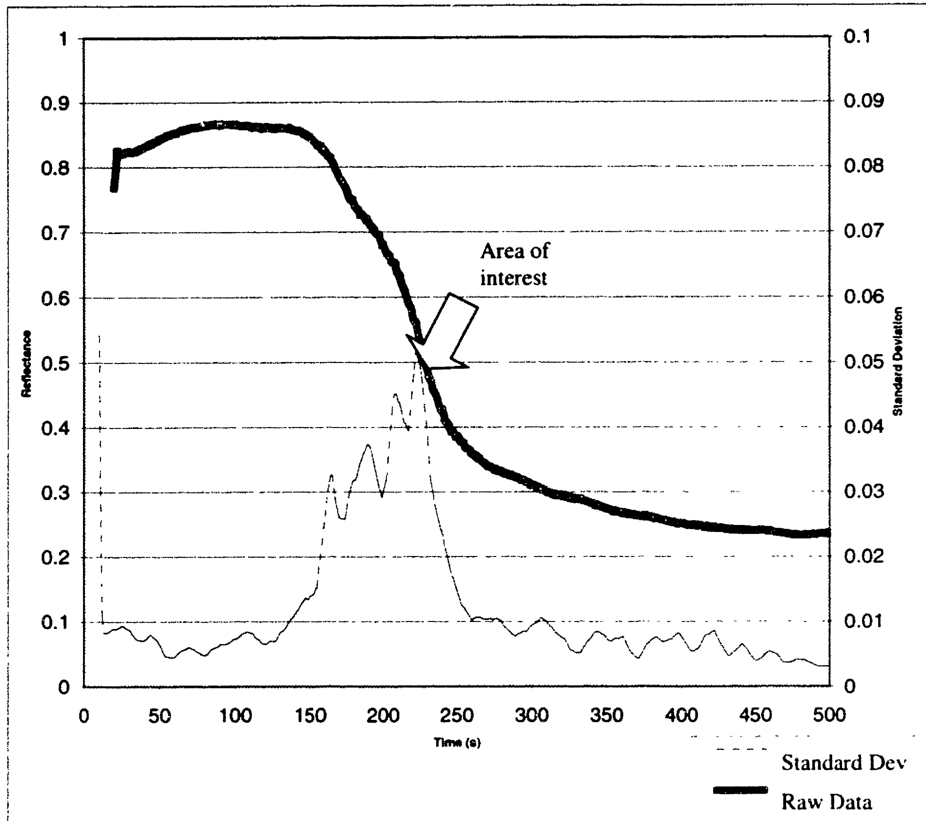

Figure 5.12 Detection by Monitoring Standard Deviation

5.4.4 Monitoring the Removal Rate

This detection method is unable to measure the *thickness* of the copper layer. However, monitoring the scattering of light caused by the surface topography at the early stages of polishing, may be an indicator of how fast the surface is being planarized. This information may be used as feedback to the wafer carrier so that pressures can be adjusted for the various pressure zones. The pressure profile created behind the wafer may help the wafer reach the planarization stage more uniformly.

Chapter 6: Conclusion

6.1 *Summary*

This thesis describes the design and implementation of an endpoint detection method for the Chemical Mechanical Polishing process. It focuses on using an optical reflectance sensor that locally measures the surface condition of a copper wafer while it is being polished. The advantage of this sensing method is the dynamic response to the changes that may occur in the polishing environment. It is also capable of identifying the non-uniform removal of copper layer.

The thesis also reviews the copper metallization processes that produce the initial surface topography on the wafer. The geometry of topography is highly dependent on trench structures that are etched into the oxide layer during the damascene process. A model is developed that explains how the surface evolves during polishing. It identifies four major surface characteristics of the wafer while polishing. These characteristics depend on the material properties of the wafer surface, and the size and shapes of the features resulting from the trench patterns. The reflectance characteristics of the various stages are monitored to identify the endpoint of polishing. Therefore, a reflectance model of the wafer surface was developed for these stages. Although, exact theoretical models for these characteristics are beyond the scope of this thesis, a basic understanding of how the reflectance is affected by these qualities has been obtained. By applying this knowledge, a general reflectance trend is found for blanket and patterned wafer polishing.

After determining the desired variable to measure, an appropriate reflectance sensor was chosen, and implemented into the polishing machine. Multiple blanket wafers were

then polished on a modified CMP test bed. The results show the ability of the sensor to monitor and detect the endpoint of the polishing process. The signal trends found during these experiments follow the trends modeled in Chapter 3. Furthermore, patterned wafers are also polished in the test bed. These results are similar to those of blanket wafer polishing. However, the distinct endpoint seen during blanket wafer polishing is not as noticeable when polishing patterned wafers. Nonetheless, the reflectance trend of the patterned wafers during polishing follows the trend modeled in Section 3.4.2.

6.2 *Possible Improvements*

The endpoint detection method presented in this thesis is capable of monitoring the surface quality of the wafer during polishing, and of detecting the endpoint. However, there are areas where improvements can be made for future designs. Currently, the optical sensor traverses across the wafer in a single arc. An area of the wafer measured at a certain distance away from the center is assumed to have similar reflectance values for equal radii. Therefore, a polish through uniformity variation can be assumed to occur in concentric rings. However, if this does not occur, it would be difficult for the detection system to determine how the wafer surface is polishing through. Thus, it may be advantageous to implement multiple sensors, which are placed at increasing distances away from the center of the pad, so that a larger area of the wafer surface can be viewed.

Another potential improvement to the machine and the detection method would be to identify the sensor position relative to the wafer surface. The slip between the wafer and carrier prevents accurate monitoring of the wafer position. However, if the rotation of the wafer is restrained, the sensor position on the wafer can be easily calculated. This would facilitate the development of expected signals that depend on pattern design.

This thesis develops a model that broadly explains the reflectance of a surface that is a function of material composition and surface profile. With complete understanding of this expected reflectance from various wafer pattern designs, the endpoint could be identified without running multiple experiments.

Until the reflectance from the surface is completely understood and an expected signal is calculated, multiple experiments that correlate the sensor signal to the surface quality need to be run. Section 5.4 discusses some signal detection schemes that are useful. However, a more rigorous test of these schemes will be needed to prove the sensor functionality in the production environment.

Finally, a more reliable and rigorous signal processing of the sensor output needs to be developed to determine the endpoint of pattern wafers. The measured sensor signals are highly dependent on the wafer pattern, which may vary substantially from one wafer to the next. A detection scheme that can account for these variations would be very beneficial.

Appendix A: Axiomatic Design

The axiomatic design methodology is a powerful tool that has the ultimate goal of establishing a science base for design activities by providing the designer with a theoretical foundation based on logical and rational thought processes and tools. It demands the clear formulation of design objectives through the establishment of functional requirements and constraints. It provides the guidance to choose the best ideas in the earlier stages in the design phase. [16]

The endpoint detection system used this methodology to accelerate and enhance the design process. It allowed the designer to understand the fundamental needs vital to produce a good design. The following pages will outline the axiomatic decomposition for the endpoint detection system. The decomposition will focus on the development of the optical sensor and its sub-components.

The FR's of the Control Remaining Thickness are as follows:

	Functional Requirements (FRs)	Design Parameters (DPs)
1	Measure condition of wafer surface	Condition sensors
2	Send stop polish signal	a. Endpoint detection algorithm b. Endpoint anticipation algorithm

Constraint Table Index	Parent	Description	Impacts: FR 1	2	3
		-- Critical Performance Specifications --			
C1a		Do not damage wafer surface	✓		
C1b		The detection must be in-situ	✓		
C1c		Cu metal wafer detection	✓		
C1d		Local detection	✓		
		-- Operational Constraints --			
C1a		Operate with slurry obstruction	✓		
C1b		Allow automated operation	✓		

$$\begin{Bmatrix} FR1 \\ FR2 \end{Bmatrix} = \begin{bmatrix} X & O \\ X & X \end{bmatrix} \begin{Bmatrix} DP1 \\ DP2 \end{Bmatrix}$$

DP1 Many possible measurement devices and methods will be explained in the next level.

DP2 An output signal from the EPD system tells the machine to stop polishing

The endpoint algorithm is coupled to the following FR's:

FR1: The stop signal is sent after the wafer surface condition is analyzed

FR1 Measure condition of wafer surface

DP1 Condition sensing sensors

	Functional Requirements (FRs)	Design Parameters (DPs)
11	Measure μ	Platen τ sensor
12	Measure acoustic emission	Audio microphone
13	Measure chemical properties	Chemistry analysis system
14	Measure electrical properties	Electrical probes
15	Local reflectance	In-situ sensor

$$\begin{Bmatrix} FR11 \\ FR12 \\ FR13 \\ FR14 \\ FR15 \end{Bmatrix} = \begin{bmatrix} X & O & O & O & O \\ O & X & O & O & O \\ O & O & X & O & O \\ O & O & O & X & O \\ X & X & O & O & X \end{bmatrix} \begin{Bmatrix} DP11 \\ DP12 \\ DP13 \\ DP14 \\ DP15 \end{Bmatrix}$$

Constraint Table Index	Parent	Description	Impacts: FR 1	2	3	4	5
		-- Critical Performance Specifications --					
C11a		Measure μ in the most direct way	✓				
C11b		Measurement method must adapt to process change	✓	✓	✓	✓	✓
		-- Operational Constraints --					
C11		Allow easy installation and use	✓	✓	✓	✓	✓
		-- Global Constraints --					
C11		Do not contact the wafer surface	✓	✓	✓	✓	✓
C12a		Require low noise surrounding		✓			
C13		Do not damage wafer internal circuits			✓	✓	
C11		Obtain measurements in-situ	✓	✓	✓	✓	✓
C15		Sensor design should not significantly affect the machine design	✓	✓	✓	✓	✓
C15		"local" is less than 1/10 the die fundamental dimension					✓

DP11 The platen τ sensor is algebraically related to the friction coefficient between the wafer and the pad. (Global detection method)

$$\mu = \left(\frac{P_{normal} A_{wafer}}{d_{offset}} \right) \tau$$

DP12 The microphone can be positioned near the wafer pad interaction to detect small changes in the acoustic signature. A change in signal can result when a rougher wafer surface becomes smoother as well as when one material is removed to expose another material. There is a change in the overall μ. (Global detection method)

DP13 The chemical analysis system can be used to analyze the chemical and particle content of the waste slurry. New materials can be introduced or reduced while polishing. For example, polishing Cu wafers results in land areas being exposed, which reduces the overall Cu concentration in the slurry. This has high dependency on the process. (Global detection method)

DP14 Electrical properties are as follows: conductance, capacitance, and impedance.
Conductance: Measures the conductivity of the wafer surface as SiO2 is polished away. It requires that an electrode touch the wafer surface.
Capacitance: Measures SiO_2 layer thickness.
Impedance: Measures amount of metal present. A small inductive coil induces a high frequency signal that reflects off of the wafer surface to give an indication of change. The reflection coefficient changes dramatically as metal is polished away. (Metal detection approach)
(Global / Local)

DP15 Optical reflectance measurement device gives the reflectance of a surface. (Local, die level detection)
The optical sensor is coupled to the following FR's:
FR1: If the sensor window changes form, it can change the τ output characteristic
FR2: The acoustic microphone may pick up additional signals due to the reflectance measurement device.

FR15 Measure local reflectance

DP15 In-situ reflectance sensor

	Functional Requirements (FRs)	Design Parameters (DPs)
151	Set sensor-wafer separation	ISS mounting mechanism
152	Measure I/I_o	Philtec sensor probe
153	Record sensor-wafer relative position	ISS position coordinating algorithm
154	Record I/I_o	ISS sampling routine

$$\begin{Bmatrix} FR11 \\ FR12 \\ FR13 \\ FR14 \end{Bmatrix} = \begin{bmatrix} X & O & O & O \\ O & X & O & O \\ O & O & X & O \\ O & O & O & X \end{bmatrix} \begin{Bmatrix} DP11 \\ DP12 \\ DP13 \\ DP14 \end{Bmatrix}$$

Constraint Table			Impacts: FR.			
Index	Parent	Description -- Critical Performance Specifications -	1	2	3	4
C151		The optimal separation distance is where change in gap does not affect the reflectance.	✓			
C152		Insulating data transport wires to minimize noise from surrounding		✓		

DP151 A mechanism that allows sensor position adjustment. Only vertical motion is allowed.

DP152 The reflectance of the wafer surface is measured using a reflectance sensor.

DP153 This algorithm estimates the location of the sensor relative to the wafer using velocity information from platen and wafer carrier motors. The algorithm will compensate for estimated slip of the wafer in the wafer carrier.
Wafer slip may occur during the sweep motion of the gantry and during the start and stop of the motor. An Adwin control system is capable of controlling the machine's overall movement and of processing the data from sensors.

DP154 The data will be taken by Adwin and stored for analysis.

FR151 Set sensor-wafer separation

DP151 ISS mounting mechanism

	Functional Requirements (FRs)	Design Parameters (DPs)
151	Mount sensor	Housing mount support structure
152	Restrict lateral motion	Vertical shaft housing
153	Restrict rotary motion	Key way
154	Adjust gap	Threaded adjust mechanism
155	Protect sensor	Sensor housing and window
156	Mount amplifier	Mounting plate

$$\begin{Bmatrix} FR151 \\ FR152 \\ FR153 \\ FR154 \\ FR155 \\ FR156 \end{Bmatrix} = \begin{bmatrix} X & O & O & O & O & O \\ O & X & O & O & O & O \\ O & O & X & O & O & O \\ O & O & O & X & O & O \\ O & O & O & O & X & O \\ O & O & O & O & O & X \end{bmatrix} \begin{Bmatrix} DP151 \\ DP152 \\ DP153 \\ DP154 \\ DP155 \\ DP156 \end{Bmatrix}$$

Constraint Table Index	Parent	Description	Impacts: FR. 1	2	3	4	5	6
		-- Critical Performance Specifications --						
C152		Align sensor vertically		✓				
C153		Limit sensor rotation to prevent cable twist			✓			
C154		Allow adjustment to optimal gap				✓		
		-- Operational Constraints --						
C154		Allow adjustment				✓		
		-- Global Constraints --						
C155a		Prevent slurry contamination					✓	
C155b		Protect sensor against any external forces					✓	

DP151 This structure mounts against the underside of the platen.
DP152 This vertical shaft restricts the lateral movements of the sensor.
DP153 The key mechanism only allows the sensor to move vertically
DP154 The adjustment mechanism changes the gap distance between the wafer surface to the sensor tip.
DP155 The metal housing and the window protect the sensor from slurry and forces.
DP156 This mechanism allows the secure mounting of the amplifier.

FR152 Measure I/I_o

DP152 Philtec sensor probe

	Functional Requirements (FRs)	Design Parameters (DPs)
1521	Measure reflectance at given gap distance	Maximum sensor range
1522	Small spot size	Philtec D6, D63, and D64 model
1523	Low noise level	Insulated wires and reduce gain

$$\begin{Bmatrix} FR1521 \\ FR1522 \\ FR1523 \end{Bmatrix} = \begin{bmatrix} X & O & O \\ X & X & O \\ X & X & X \end{bmatrix} \begin{Bmatrix} DP1521 \\ DP1522 \\ DP1523 \end{Bmatrix}$$

Constraint Table Index	Parent	Description	Impacts: FR. 1	2	3	4	5	6
		-- Critical Performance Specifications --						
C1521		The maximum gap distance must not be exceeded	✓					

DP151 This is the maximum distance where the sensor will no longer correctly measure the reflectance of the wafer surface

DP152 Choosing a model offers specific features
D6- smaller spot size, but restricts the gap distance to ~50mils.
D64- larger spot size, but allows the gap distance to be ~250mils.

FR3 Send stop polish signal

DP3 a. Endpoint detection algorithm

b. Anticipation algorithm

	Functional Requirements (FRs)	Design Parameters (DPs)
31	Estimate wafer polish completion	Polish state algorithm
32	Send stop signal	Stop flag to ARP controller

$$\begin{Bmatrix} FR31 \\ FR32 \end{Bmatrix} = \begin{bmatrix} X & O \\ O & X \end{bmatrix} \begin{Bmatrix} DP31 \\ DP32 \end{Bmatrix}$$

Constraint Table			Impacts: FR			
Index	Parent	Description	1	2	3	4
		-- Critical Performance Specifications --				
C31		Reduce over-polishing of wafer	✓			
C32		Stop signal must be generated and sent within a 3 second window		✓		

DP31 This algorithm estimates the level of polishing done to the wafer using measured parameters. At the simplest level, polish state is a function of friction, reflectance, and time.

DP32 When the measured parameters indicate that the polish is complete, a signal will be sent to the ARP to stop the polishing process.

Note: A simple endpoint detection algorithm will compare the average reflectance from the wafer surface to a threshold value that may trigger the end of polishing. The next level of signal processing will anticipate the stop rather than simply waiting for the absolute signal. This may be accomplished by measuring the rate of SiO_2 exposed from one revolution to the next. On the other hand, the characteristics of the wafer's features may be used as a stop signal. This may involve using statistical methods to anticipate the output signal that change with varying density fields.

Appendix B: Sensor Holder Design

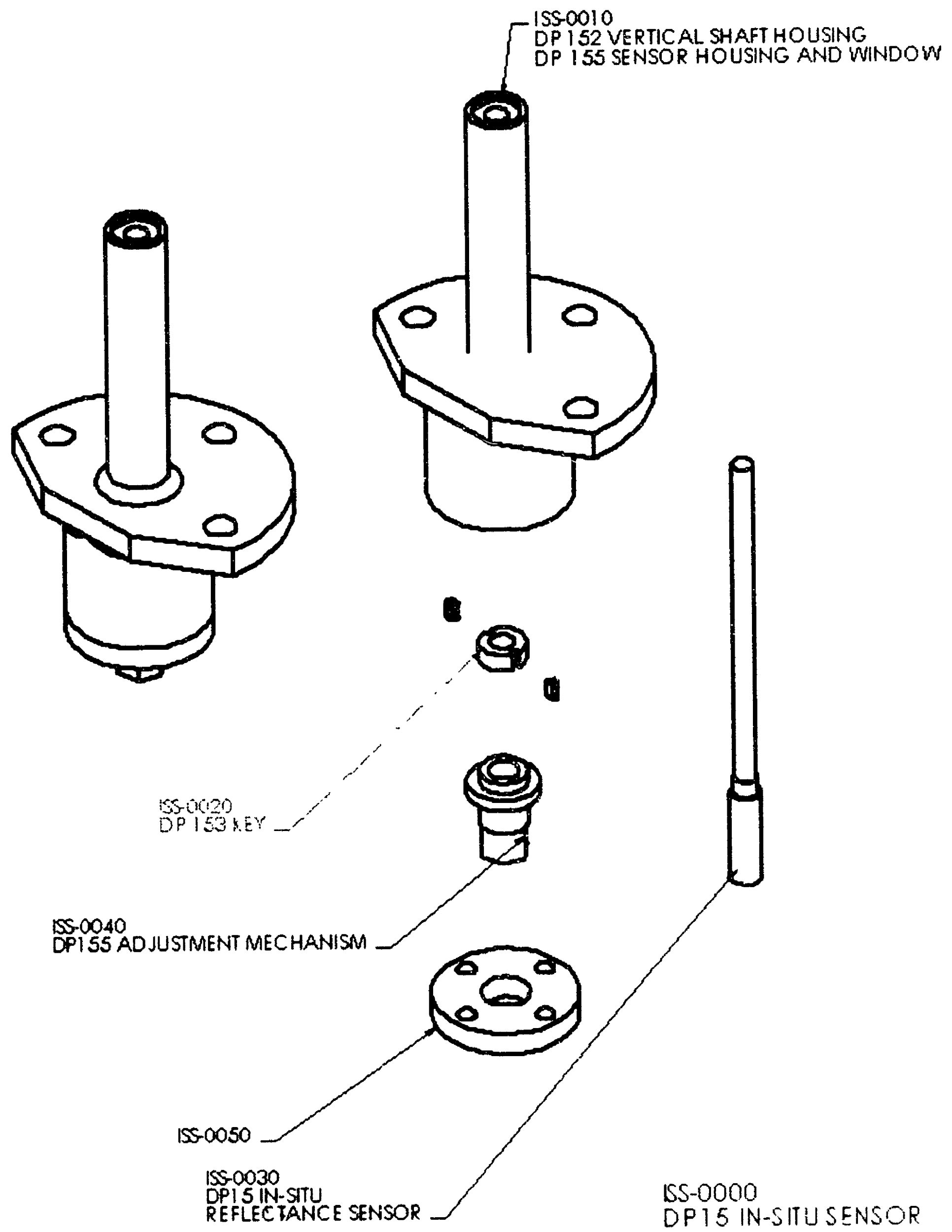

Figure A. 1 Assembly Exploded View of Sensor Holder

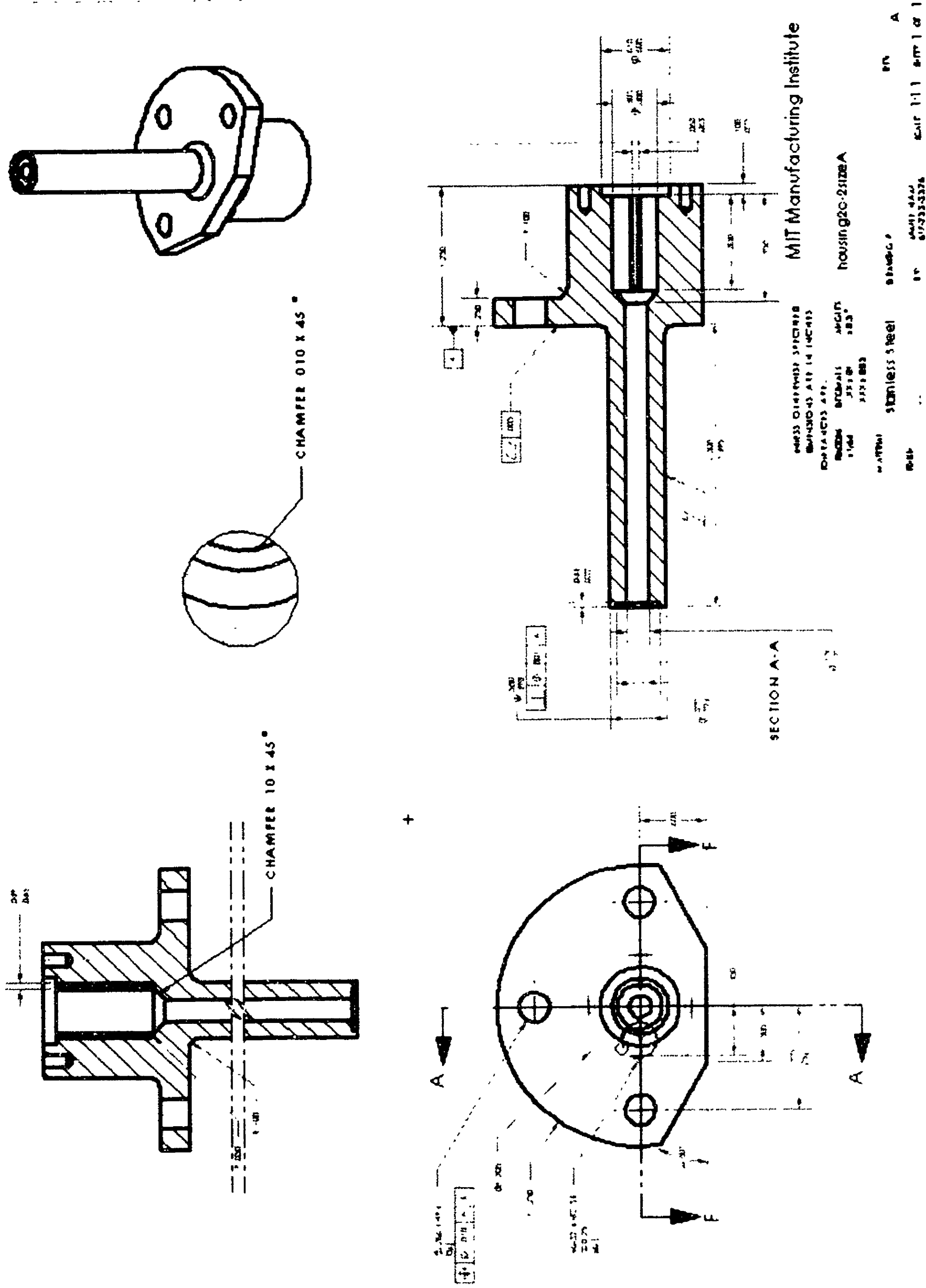

Figure A. 2 Sensor Housing

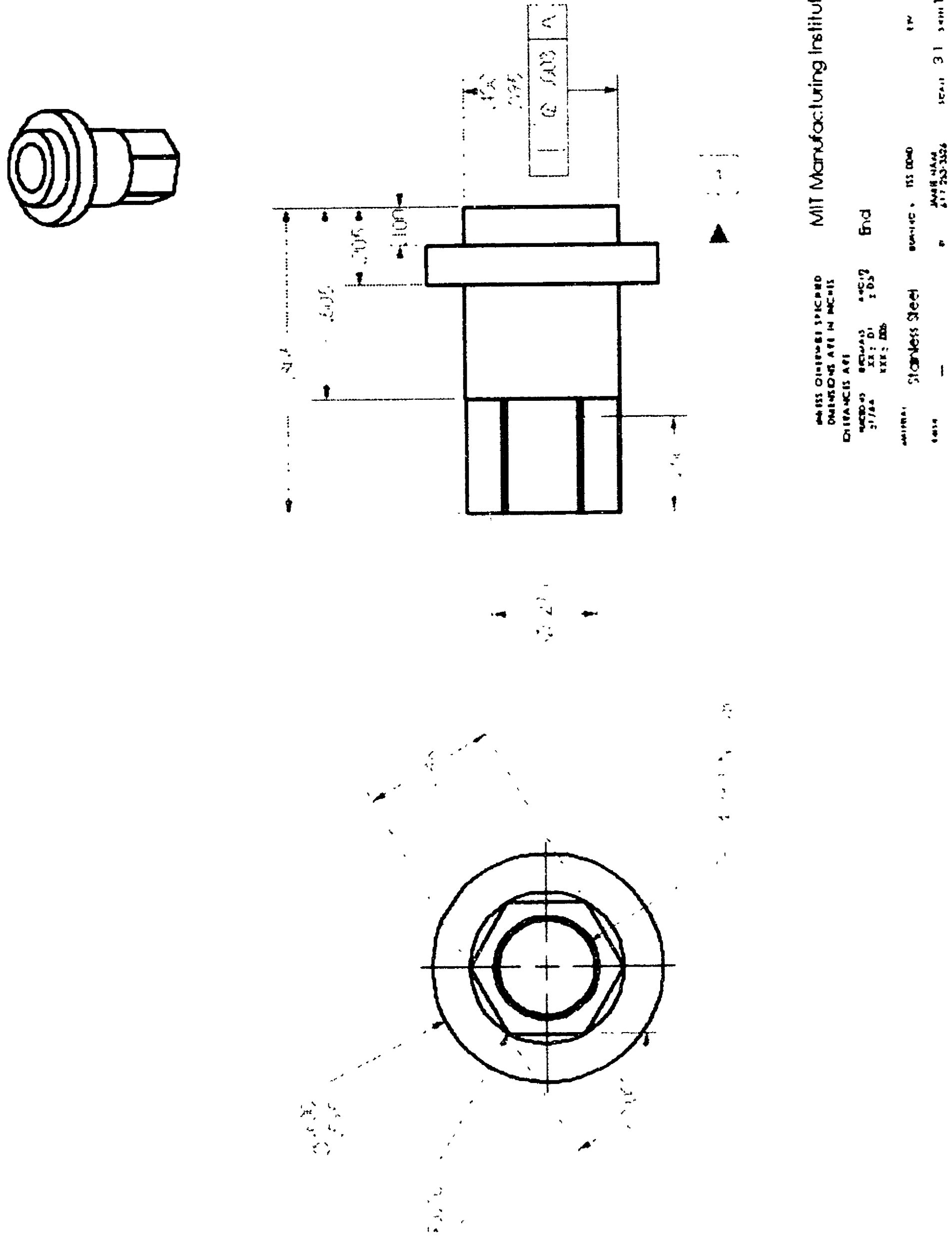

Figure A. 3 Positioning Nut

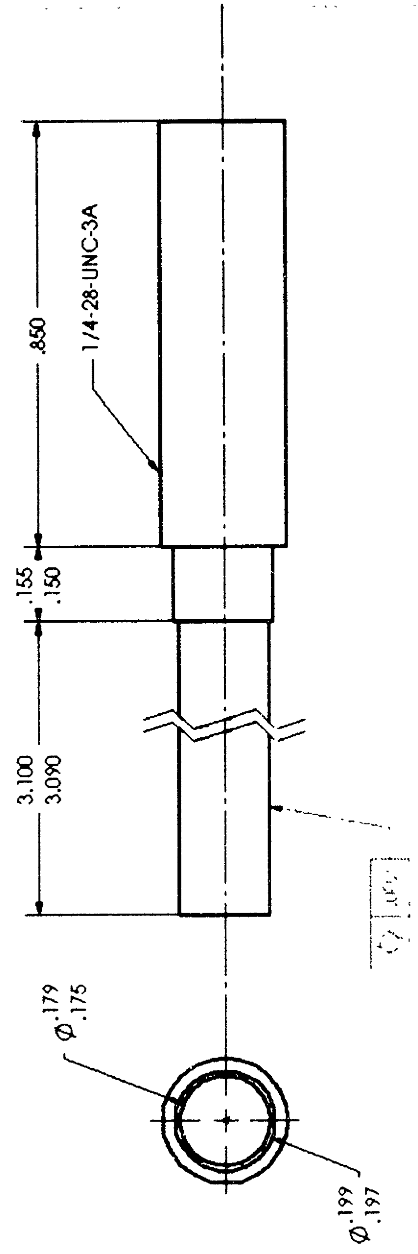

Figure A. 4 Sensor Tip

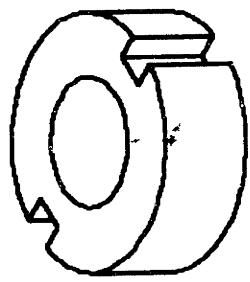

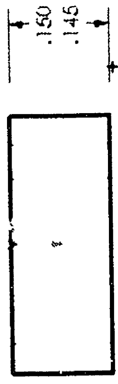

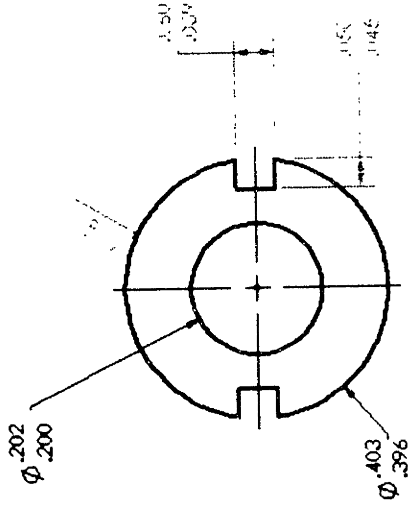

MIT Manufacturing Institute

Key

Stainless Steel

Figure A. 5 Sensor Restraining Key A

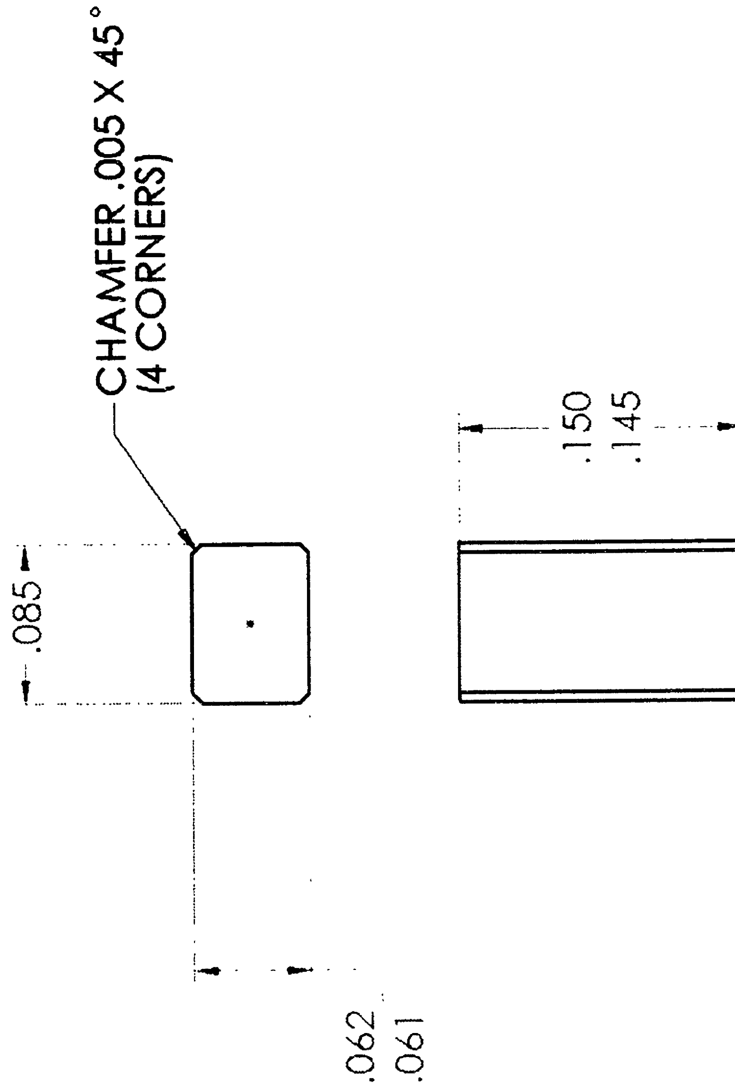

Figure A. 6 Sensor Restraining Key B

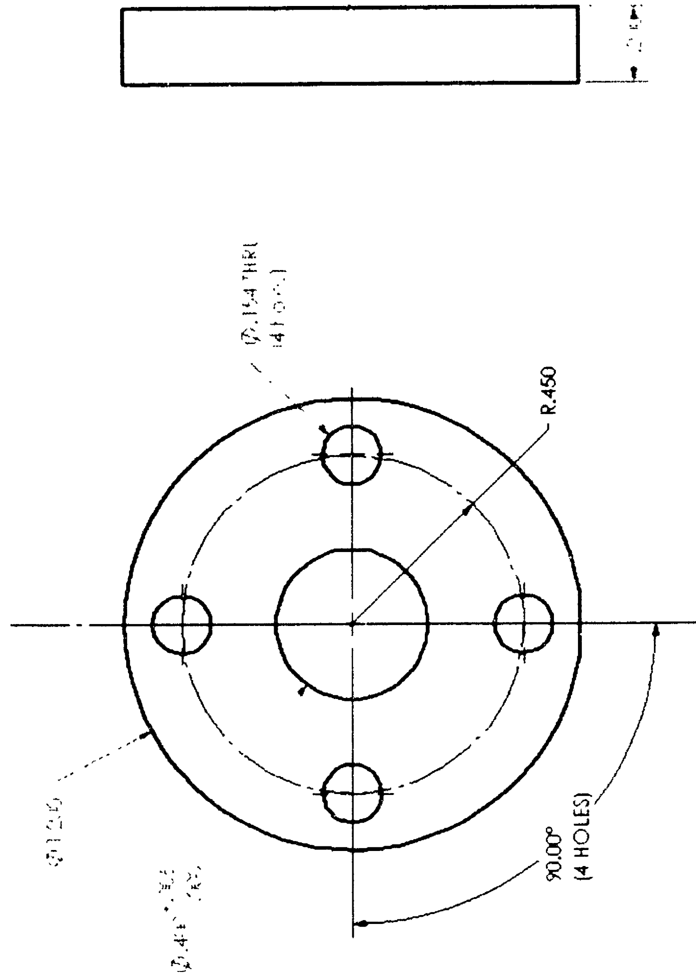

Figure A. 7 Locking Mechanism

SECTION A-A

MIT Manufacturing Institute

sensor bracket

Stainless Steel

Figure A. 8 Wall Mount

References

[1] Peter Singer, "Tantalum, Copper and Damascene: The Future of Interconnects," *Semiconductor International,* Vol.21, No.6, June 1998.

[2] Peter Singer, "Dual-damascene challenges dielectric etch," *Semiconductor International,* Vol.22, No.9, Aug. 1999.

[3] Ruth Dejule, "CMP grows in sophistication," *Semiconductor International,* Vol.21, No.13, Nov. 1998.

[4] G. Dishon, M. Finarov, R. Kipper, "Monitoring Choices of CMP Planarization Processes," *VMIC Specialty Conferences, 2nd International CMP Planarization Conference,* Santa Clara, CA, Feb 1997.

[5] Thomas Bibby, Karey Holland, "Endpoint detection for CMP," *Journal of Electronic Materials,* Vol.27, Vo.10, Oct 1998.

[6] Gurtej Sandhu, Laurence Schultz, Trung Doan, U.S. Patent #5,036,015, July 30, 1991.

[7] Carter Kaanta, Michael Leach, U.S. Patent #4,793,895, December 27, 1988.

[8] Michael Leach, et al, U.S. Patent #5,213,655, May 25, 1993.

[9] Gabriel Miller, Eric Wagner, U.S. Patent #5,081,421, January 14, 1992.

[10] Scott Meikle, Trung Doan, U.S. Patent #5,439,551, August 8, 1995.

[11] Shyam Murarka, Ronald Gutmann, David Duquette, Joseph Steigerwald, U.S. Patent #5,637,185, June 10, 1997.

[12] Daniel Koos, Scott Meikle, U.S. Patent #5,413,941, May 9, 1995.

[13] Petr Beckmann, Andre Spizzichino, "The Scattering of Electromagnetic Waves from Rough Surfaces," Oxford, Pergamon Press, 1963.

[14] Milton Abramowitz, Irene Stegun, "Handbook of Mathematical Functions with Formulas, Graphs, and Mathematical Tables," National Bureau of Standards Applied Mathematics Series 55, June 1964.

[15] David R. Lide, "Handbook of Chemistry and Physics," CRC Press, Inc. 7th edition, June 1996.

[16] Nam P. Suh, "Axiomatic Design: Advances and Application," Oxford University Press, 1998.

THESIS PROCESSING SLIP

FIXED FIELD: ill. ______ name ______

index ______ biblio ______

▶ COPIES: Archives Aero Dewey Eng Hum

Lindgren Music Rotch Science

TITLE VARIES: ▶☐ ______

NAME VARIES: ▶☐ ______

IMPRINT: (COPYRIGHT) ______

▶ COLLATION: ______

▶ ADD: DEGREE: ______ ▶ DEPT.: ______

SUPERVISORS: ______

NOTES:

cat'r date

page

▶ DEPT. ______

▶ YEAR: ______ ▶ DEGREE: ______

▶ NAME: ______